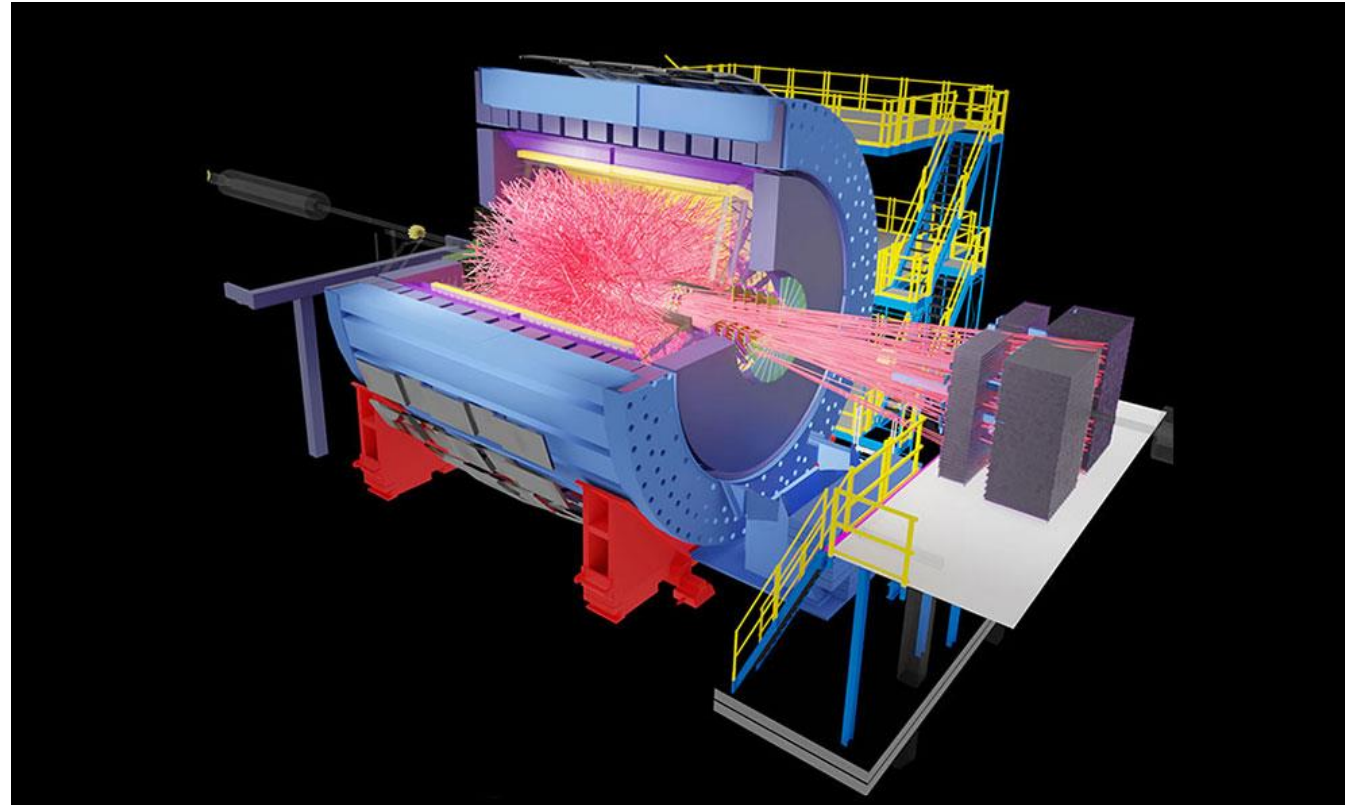


QCD under extreme conditions – present and future STAR's perspective

Lijuan Ruan (BNL)

September 20, 2025

RHIC and STAR



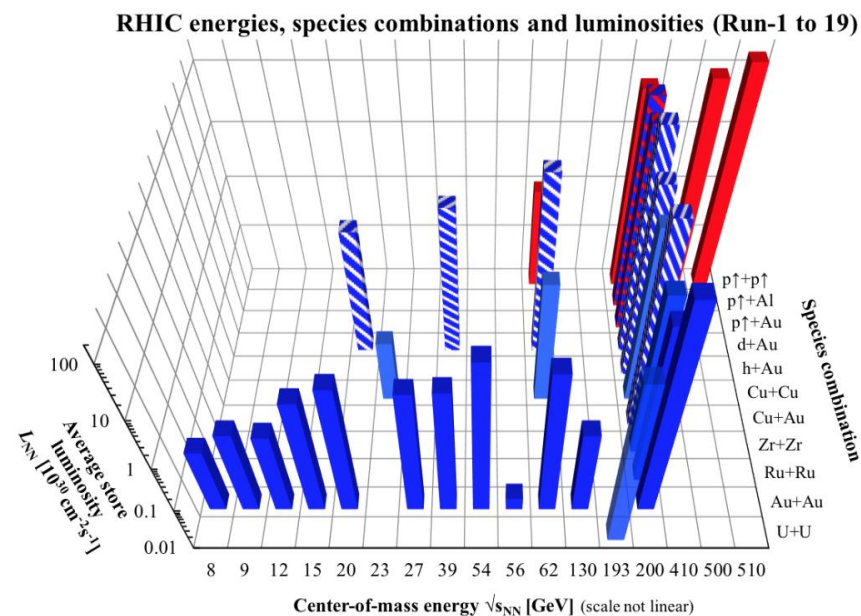
25 years of RHIC operation

It has been an amazing journey

Evolution of the STAR Detector

major upgrades over the last twenty years to improve particle identification and vertex reconstruction, and is still evolving with an extension to forward rapidity as of today. pioneered in using new technologies: MRPC, MAPS, GEM and siPM.

Estimate 35M(initial) +75M(upgrades)\$.



Detector	primary functions	DOE+(in-kind)	year
TPC+Trigger	$ \eta < 1$ Tracking		1999-
Barrel EMC	$ \eta < 1$ jets/ $\gamma/\pi^0/e$		2004-
FTPC	forward tracking	(Germany)	2002-2012
L3	Online Display	(Germany)	2000-2012
SVT/SSD	V0/charm	(France)	2004-2007
PMD	forward photons	(India)	2003-2011
EEMC	$1 < \eta < 2$ jets/ π^0/e	(NSF)	2005-
Roman Pots	diffractive		2009-
TOF	PID	(China)	2009-
FMS/Preshower	$2.5 < \eta < 4.2$	(Russia)	2008-2017
DAQ1000	x10 DAQ rate		2008-
HLT	Online Tracking	(China/Germany)	2012-
FGT	$1 < \eta < 2$ W^\pm		2012-2013
GMT	TPC calibration		2012-
HFT/SSD	open charm	(France/UIC)	2014-2016
MTD	muon ID	(China/India)	2014-
EPD	event plane	(China)	2018-
RHICf	$\eta > 5$ π^0	(Japan)	2017
iTPC	$ \eta < 1.5$ Tracking	(China)	2019-
eTOF	$-2 < \eta < -1$ PID	(Germany/China)	2019-
FCS	$2.5 < \eta < 4$ calorimeter	(NSF)	2021-
FTS	$2.5 < \eta < 4$ Tracking	(NCKU/SDU)	2021-

2

TOF/DAQ1000 (2010)
PID, Beam Energy Scan I

HFT/MTD (2014)
Heavy flavor/quarkonia

iTPC/eTOF/EPD (2019)
Beam Energy Scan II

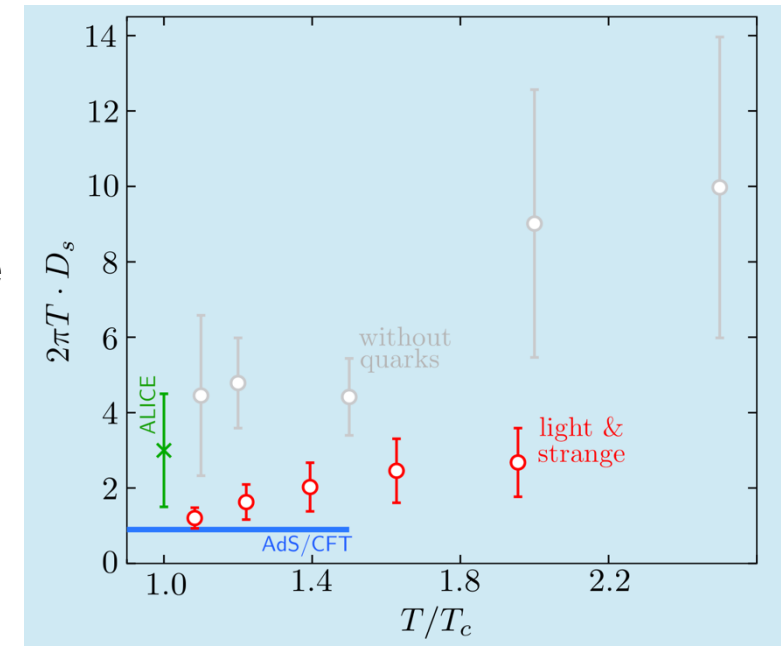
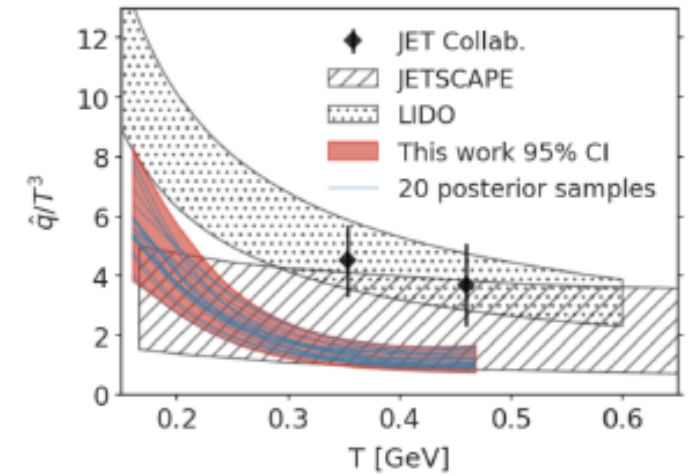
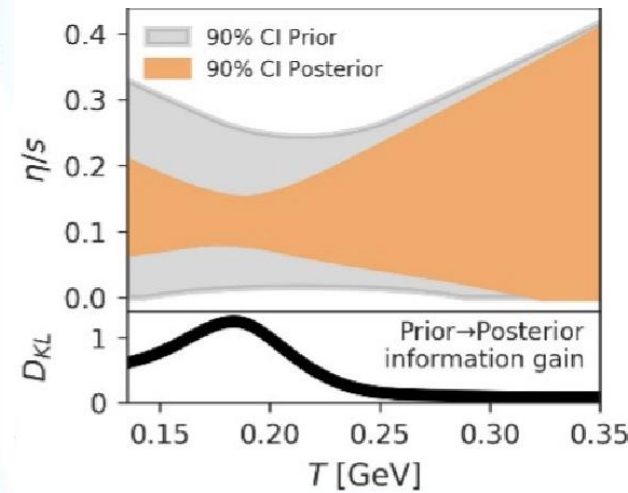
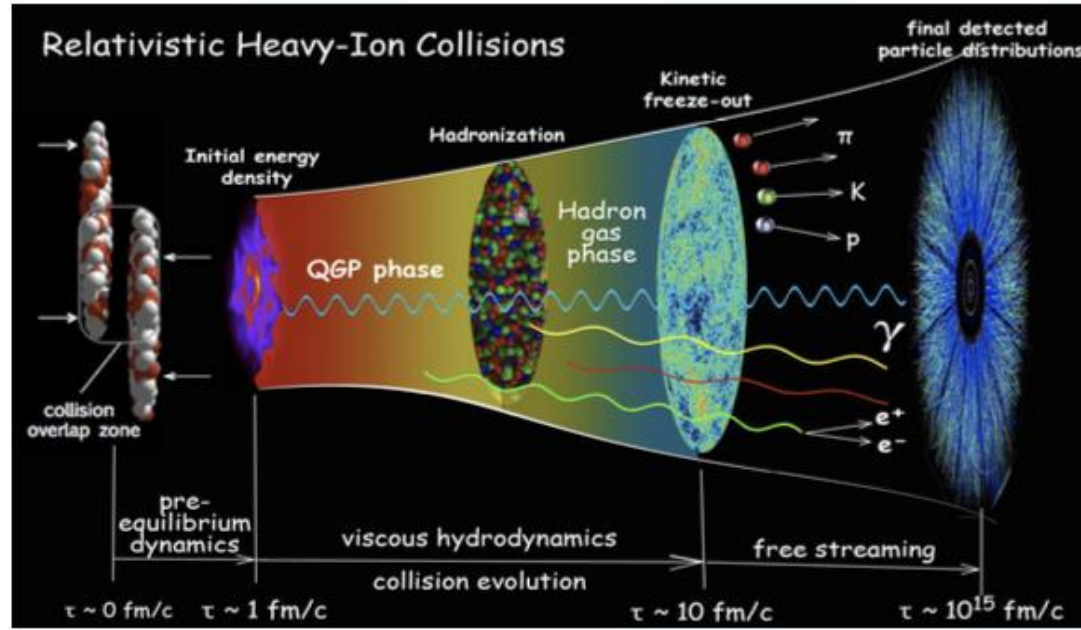
FCS/FTS (2022)
DAQ5k (2023)
Forward physics programs
in cold and hot QCD

25 years of operation, major successful upgrades, vibrant physics programs

386 published papers, 343 PhD and 34 MS theses

The properties of perfect liquid

The 2023 NSAC Long Range Plan for Nuclear Science



Essential questions to be addressed:

1. How do the fundamental interactions between quarks and gluons lead to the perfect fluid behavior of the quark-gluon plasma?
2. What are the limits on the fluid behavior of matter?
3. What are the properties of QCD matter?
4. What is the nature of the transition from QGP to hadronic matter?
5. Does a QCD critical point exist, analogous to the critical point in the water–vapor–ice phase diagram?

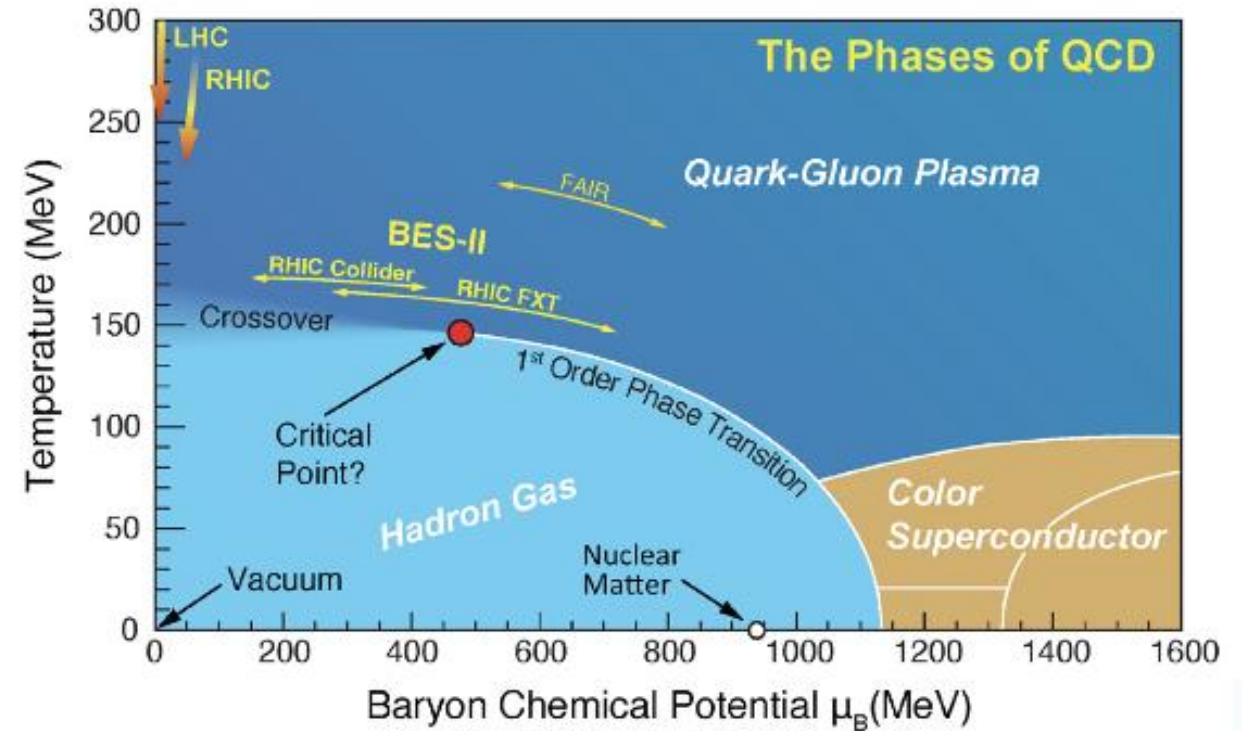
The phases of QCD matter

Lattice QCD: crossover chiral transition at $\mu_B < 3 \text{ T}$

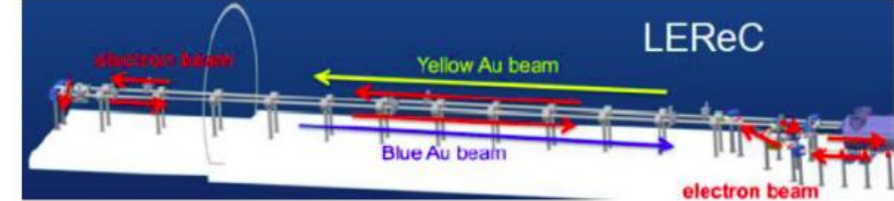
At top RHIC and LHC energies, measurements consistent with a smooth crossover chiral transition

Change T and μ_B by varying the collision energy:

- Search for the critical point
- Search for the first-order phase transition
- Search for the threshold of QGP formation

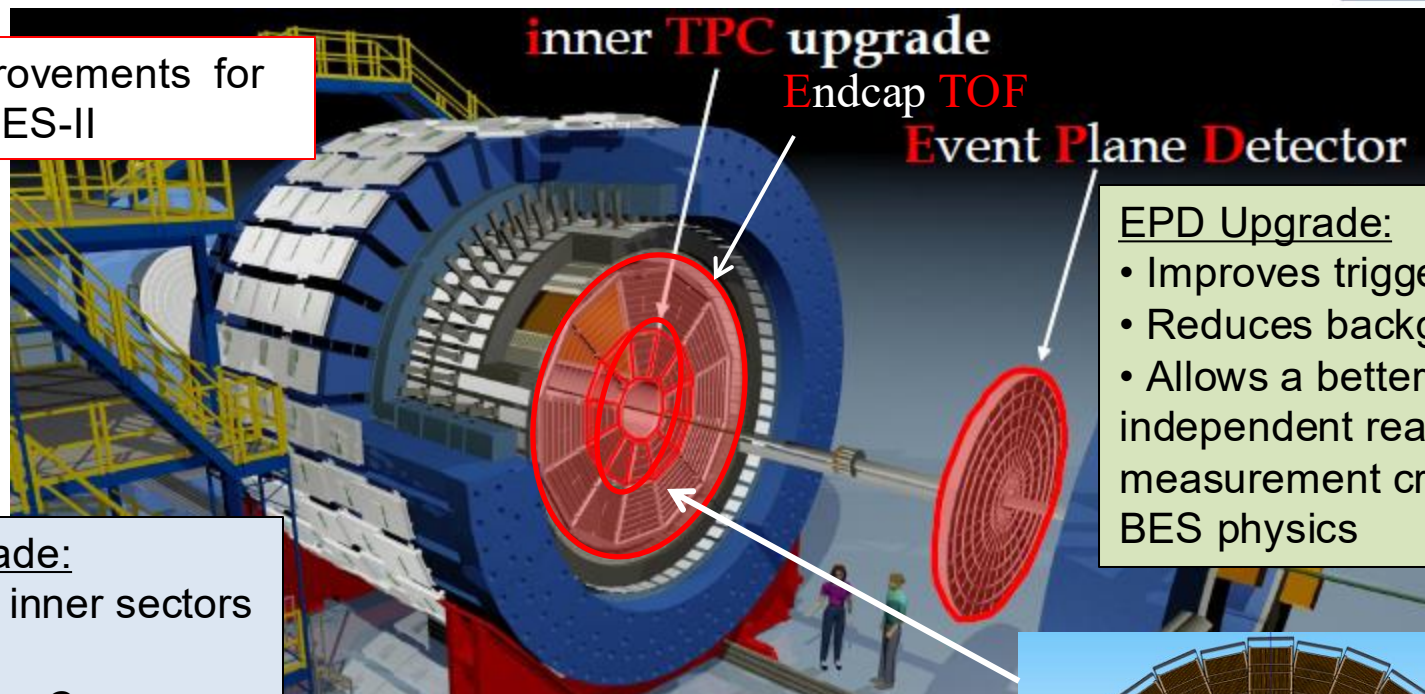


RHIC BES-II upgrades



LEReC – Low Energy RHIC electron Cooling

Major improvements for
BES-II



iTPC Upgrade:

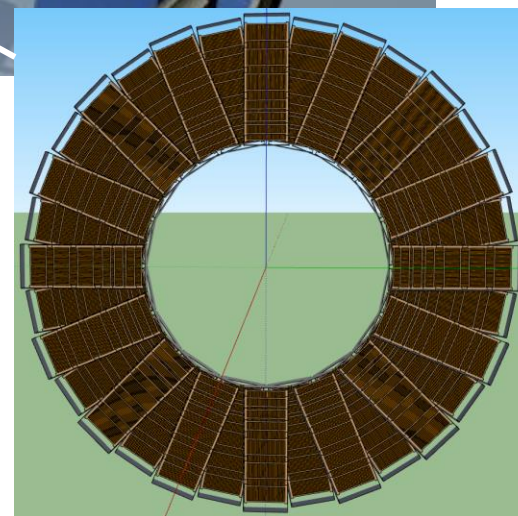
- Replaced inner sectors of the TPC
- Continuous Coverage
- Improves dE/dx
- Extends η coverage from 1.0 to 1.5
- Lowers p_T cut from 125 MeV/c to 60 MeV/c

EPD Upgrade:

- Improves trigger
- Reduces background
- Allows a better and independent reaction plane measurement critical to BES physics

EndCap TOF Upgrade:

- Rapidity coverage is critical
- PID at $\eta = 1$ to 1.5
- Improves the fixed target program
- Provided by CBM-FAIR



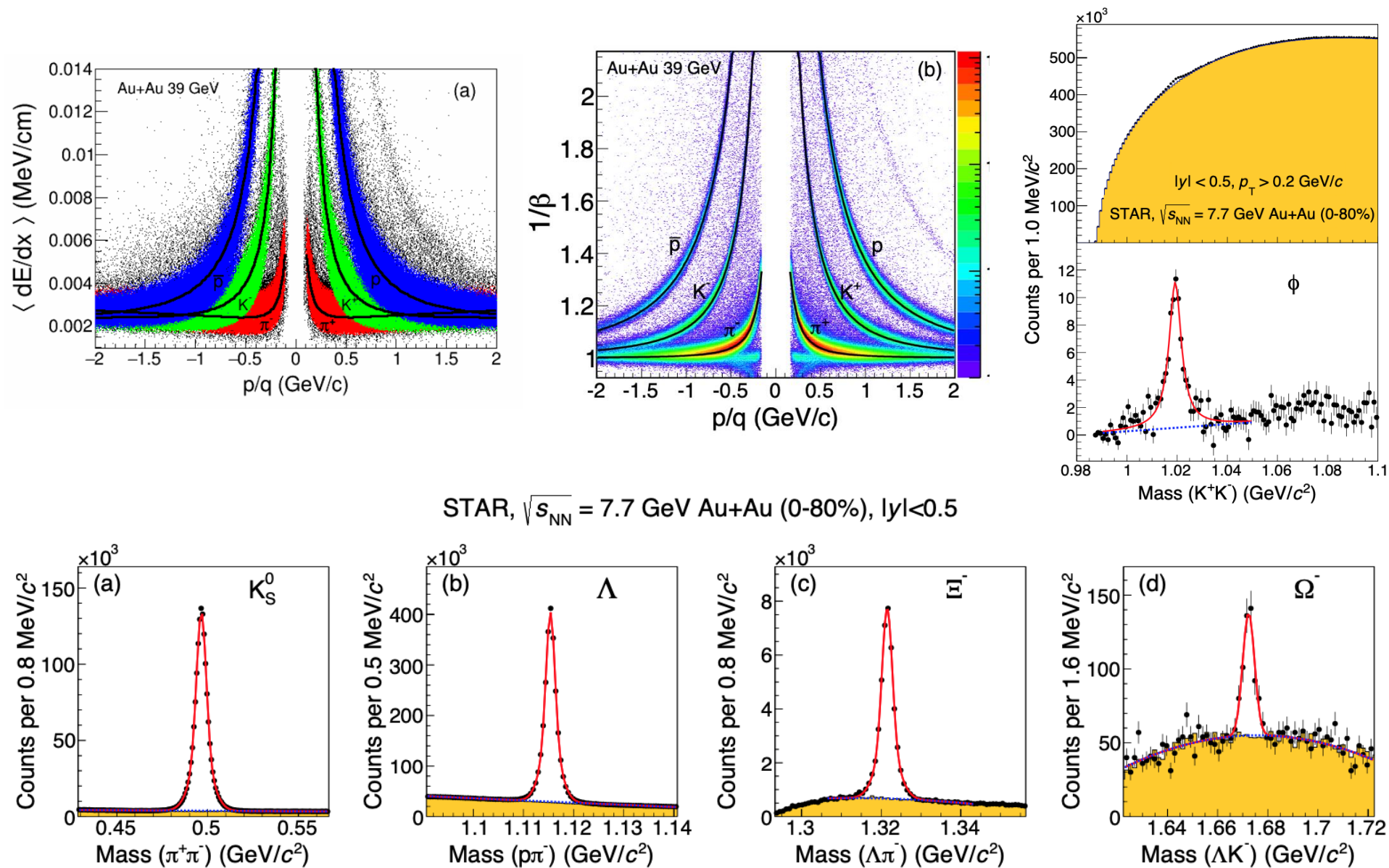
BES-II datasets (2019-2021)

Au+Au Collisions at RHIC							
Collider Runs				Fixed-Target Runs			
	$\sqrt{s_{NN}}$ (GeV)	#Events	μ_B		$\sqrt{s_{NN}}$ (GeV)	#Events	μ_B
1	200	380 M	25 MeV	1	13.7 (100)	50 M	280 MeV
2	62.4	46 M	75 MeV	2	11.5 (70)	50 M	316 MeV
3	54.4	1200 M	85 MeV	3	9.2 (44.5)	50 M	372 MeV
4	39	86 M	112 MeV	4	7.7 (31.2)	260 M	420 MeV
5	27	585 M	156 MeV	5	7.2 (26.5)	470 M	440 MeV
6	19.6	595 M	206 MeV	6	6.2 (19.5)	120 M	490 MeV
7	17.3	256 M	230 MeV	7	5.2 (13.5)	100 M	540 MeV
8	14.6	340 M	262 MeV	8	4.5 (9.8)	110 M	590 MeV
9	11.5	257 M	316 MeV	9	3.9 (7.3)	120 M	633 MeV
10	9.2	160 M	372 MeV	10	3.5 (5.75)	120 M	670 MeV
11	7.7	104 M	420 MeV	11	3.2 (4.59)	200 M	699 MeV
				12	3.0 (3.85)	260 + 2000 M	750 MeV

A broad μ_B coverage: $25 < \mu_B < 750$ MeV

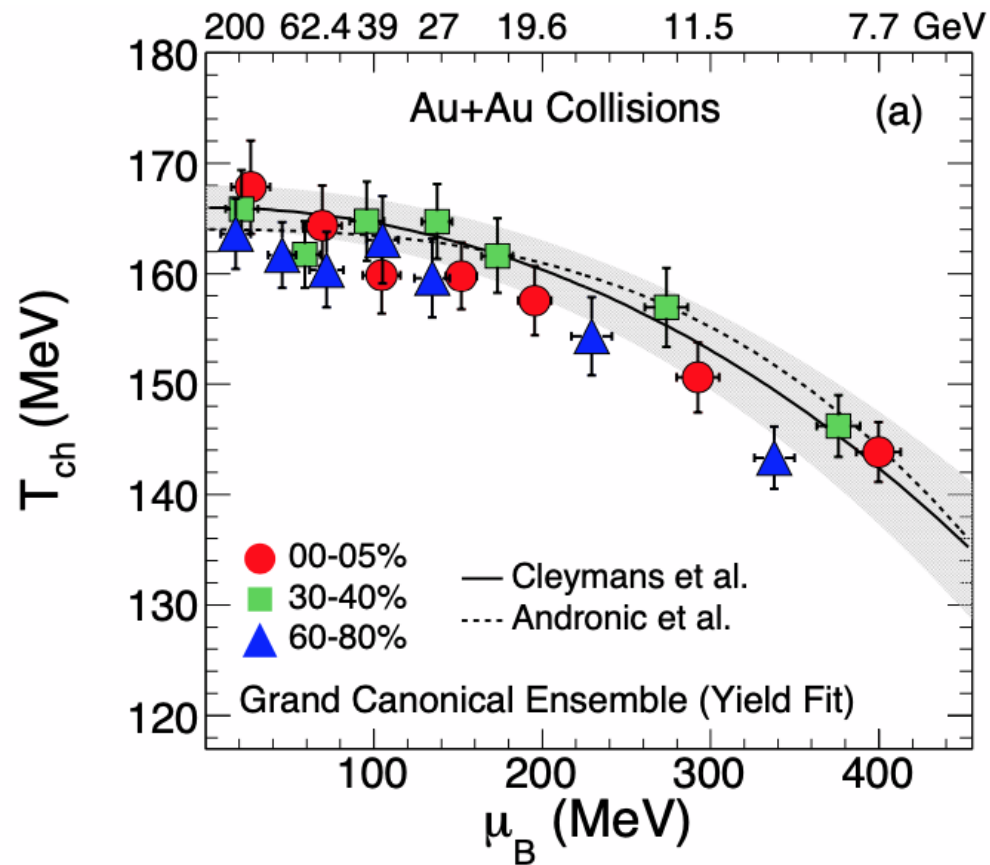
BES-II data collected at RHIC cover a broad and interesting range of μ_B for the critical point search

Particle identification with TPC+TOF



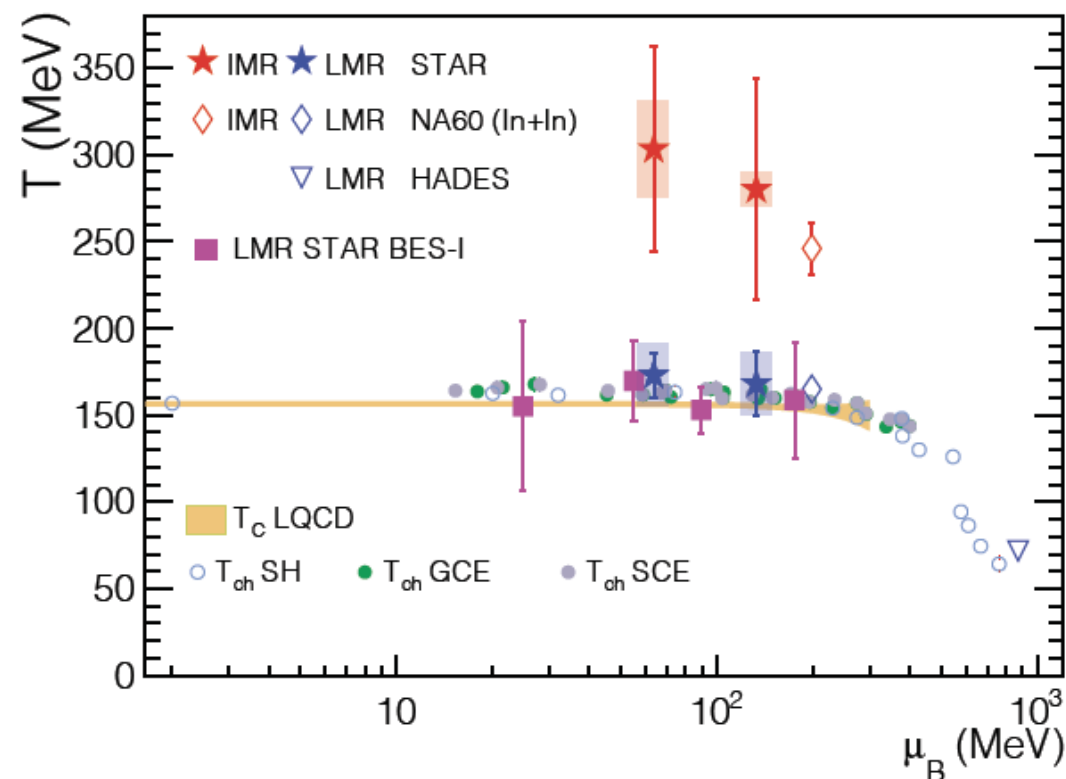
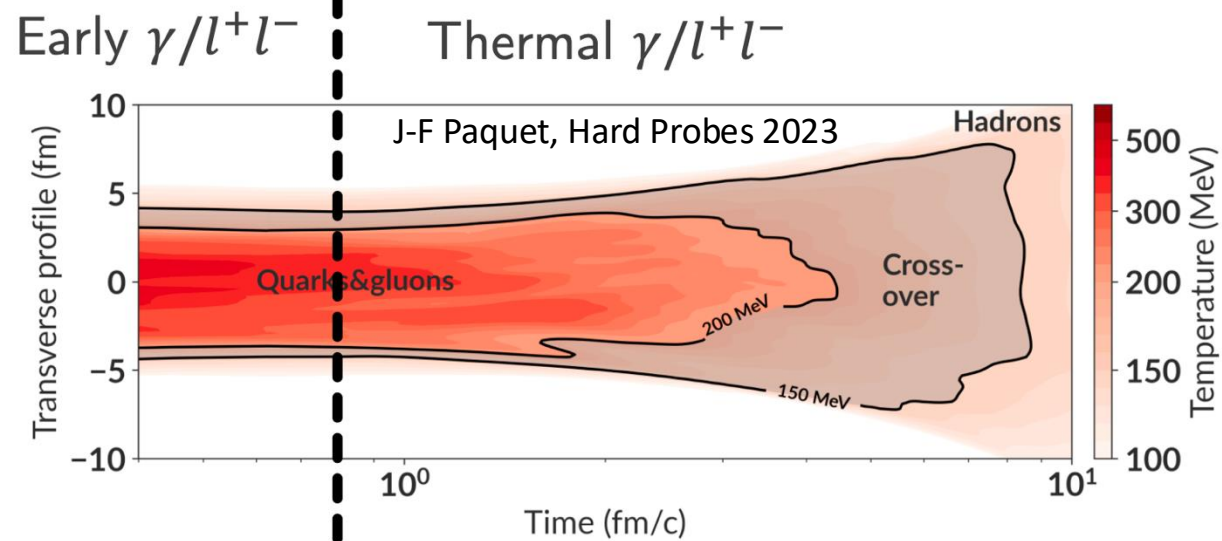
Locate T and μ_B

Phys. Rev. C 96 (2017) 44904



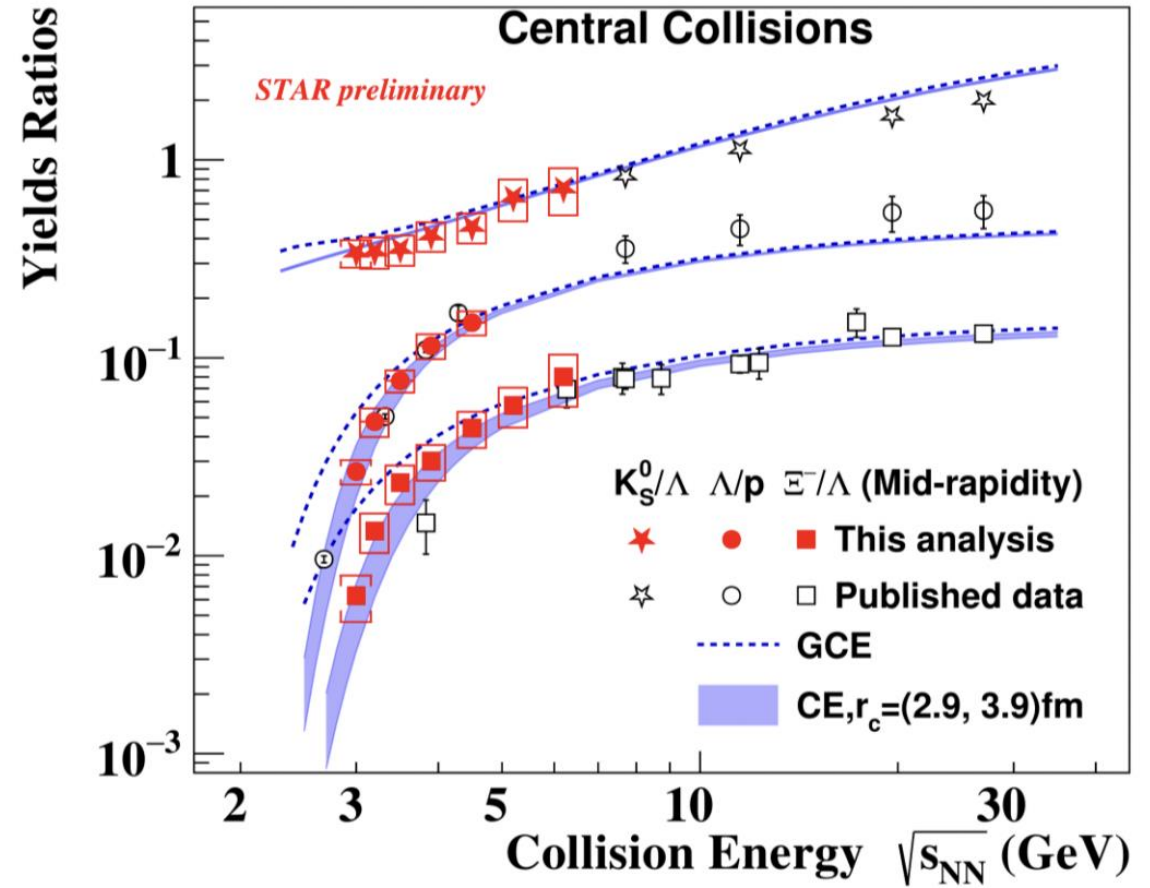
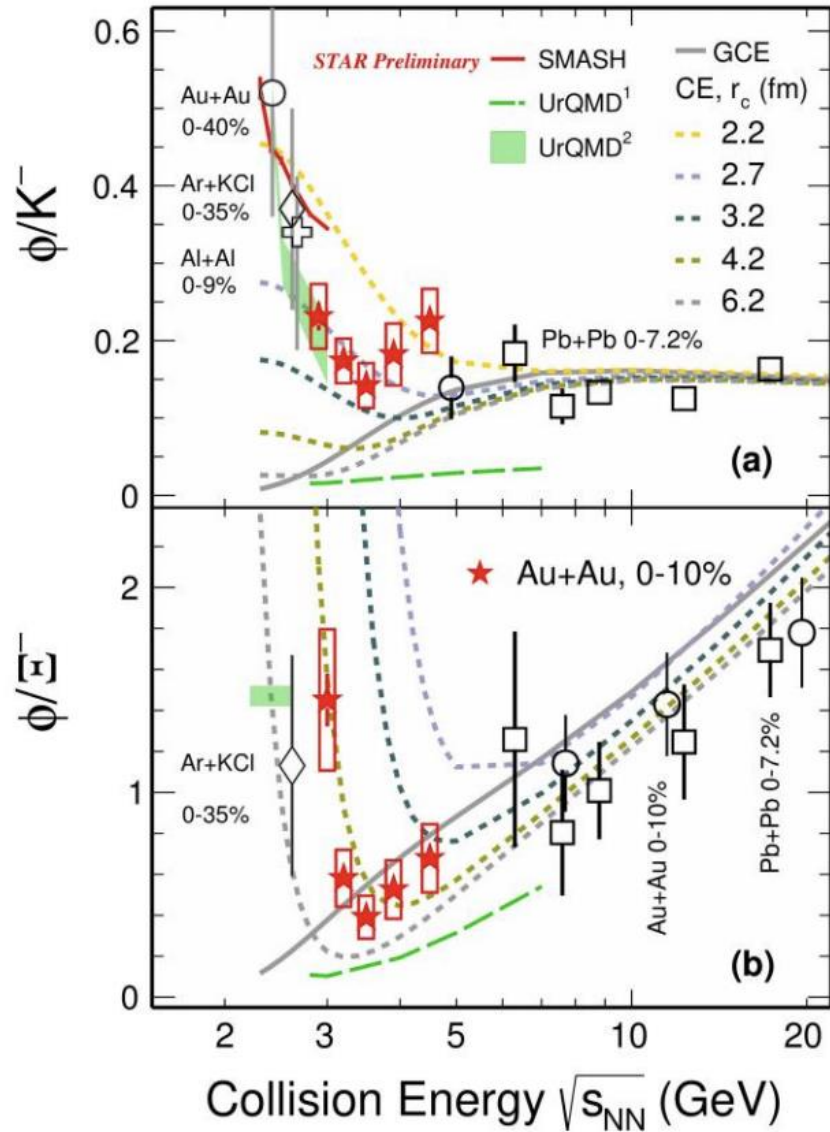
$\pi^\pm, K^\pm, p, \bar{p}, \Lambda, \bar{\Lambda}, \Xi, \text{ and } \bar{\Xi}.$

$\pi^-/\pi^+, \bar{K}^-/K^+, \bar{p}/p, \bar{\Lambda}/\Lambda, \bar{\Xi}/\Xi, K^-/\pi^-, \bar{p}/\pi^-, \Lambda/\pi^-,$
and $\bar{\Xi}/\pi^-.$



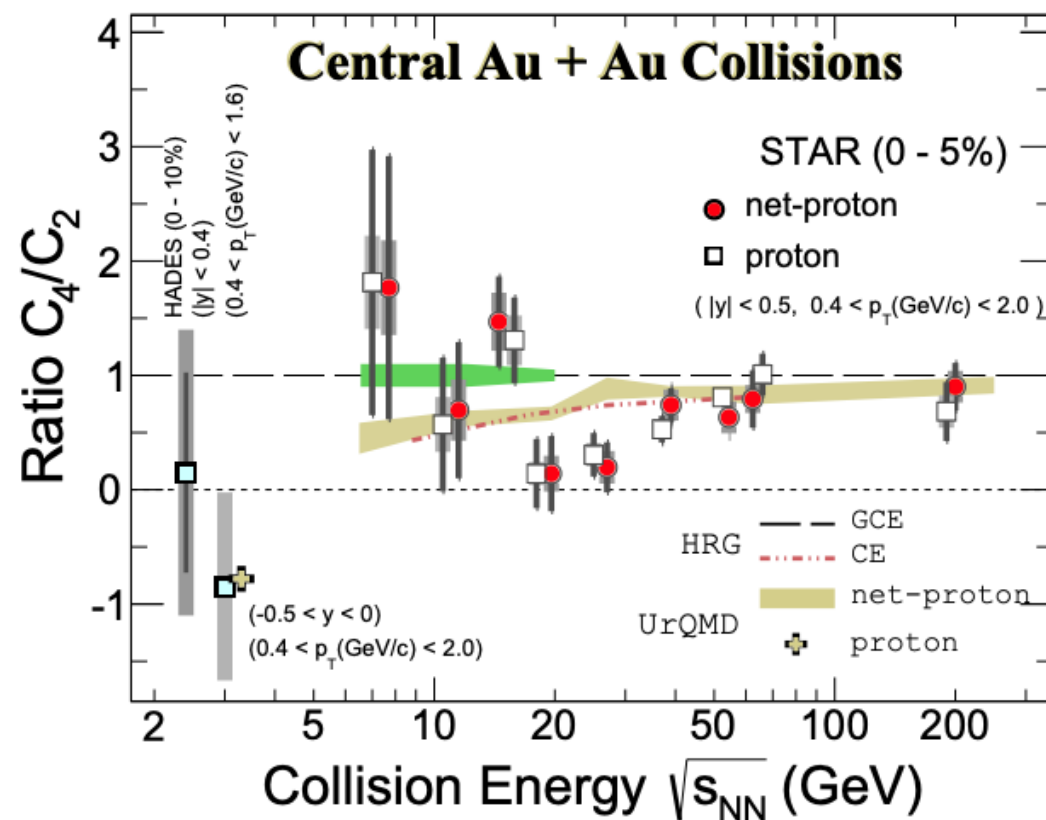
arXiv: 2402.01998, submitted to Nature Communications

Strange hadron production



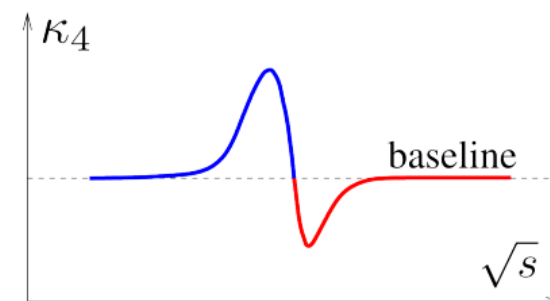
Strange hadron yield ratios deviate from Grand Canonical Ensemble expectations at collision energies below 5 GeV.

Net-proton higher moments from BES-I and at 3 GeV from FXT (2018)



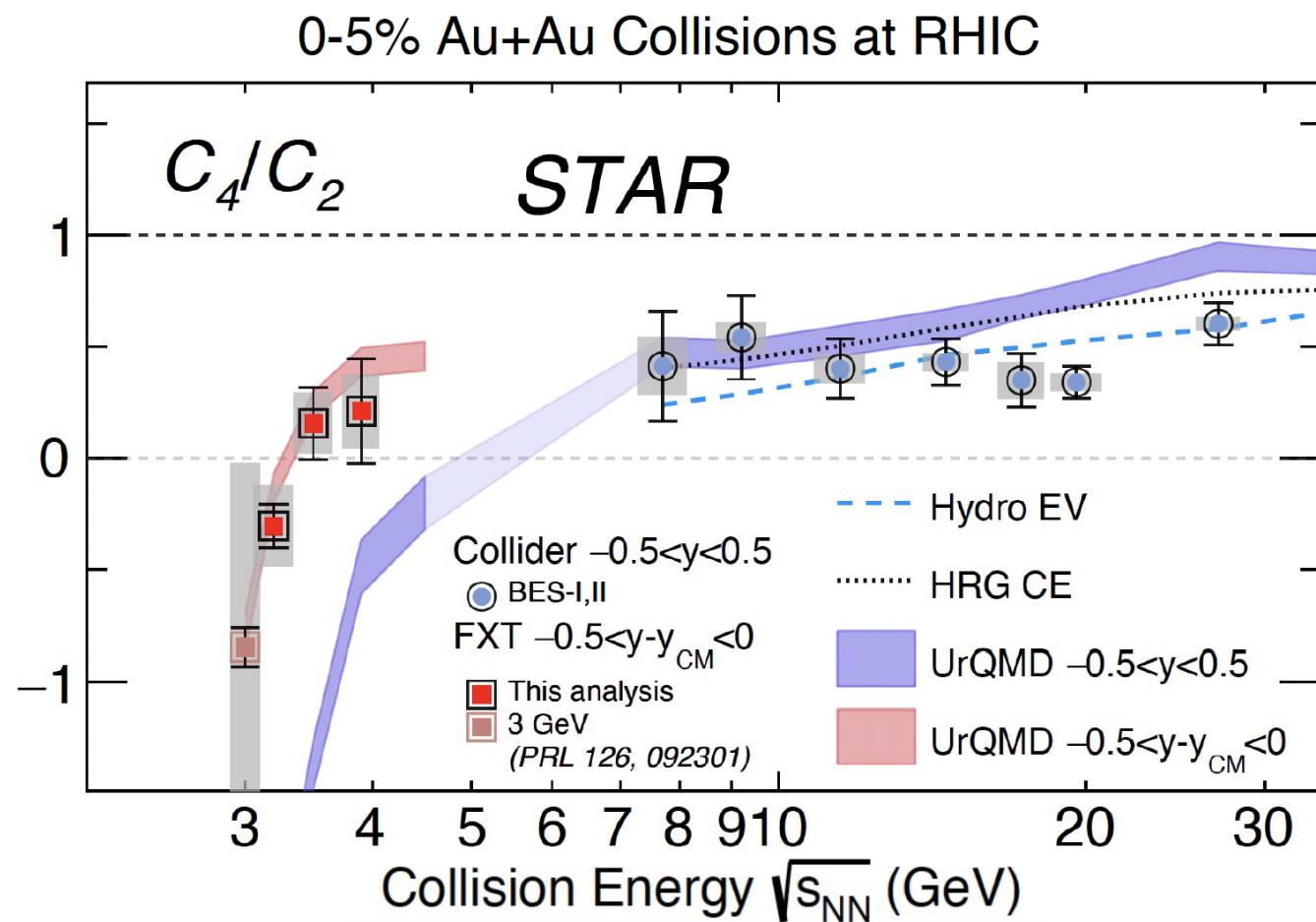
BES-I: PRL 126 (2021) 092301

3 GeV data: PRL 128 (2022) 202303



- Non-monotonic energy dependence in central Au+Au collisions (3.1σ)
- Strong suppression in proton C_4/C_2 at 3 GeV
 - consistent with UrQMD hadronic transport model calculation

Net-proton higher moments from BES-II



Collider mode:
arXiv: 2504.00817

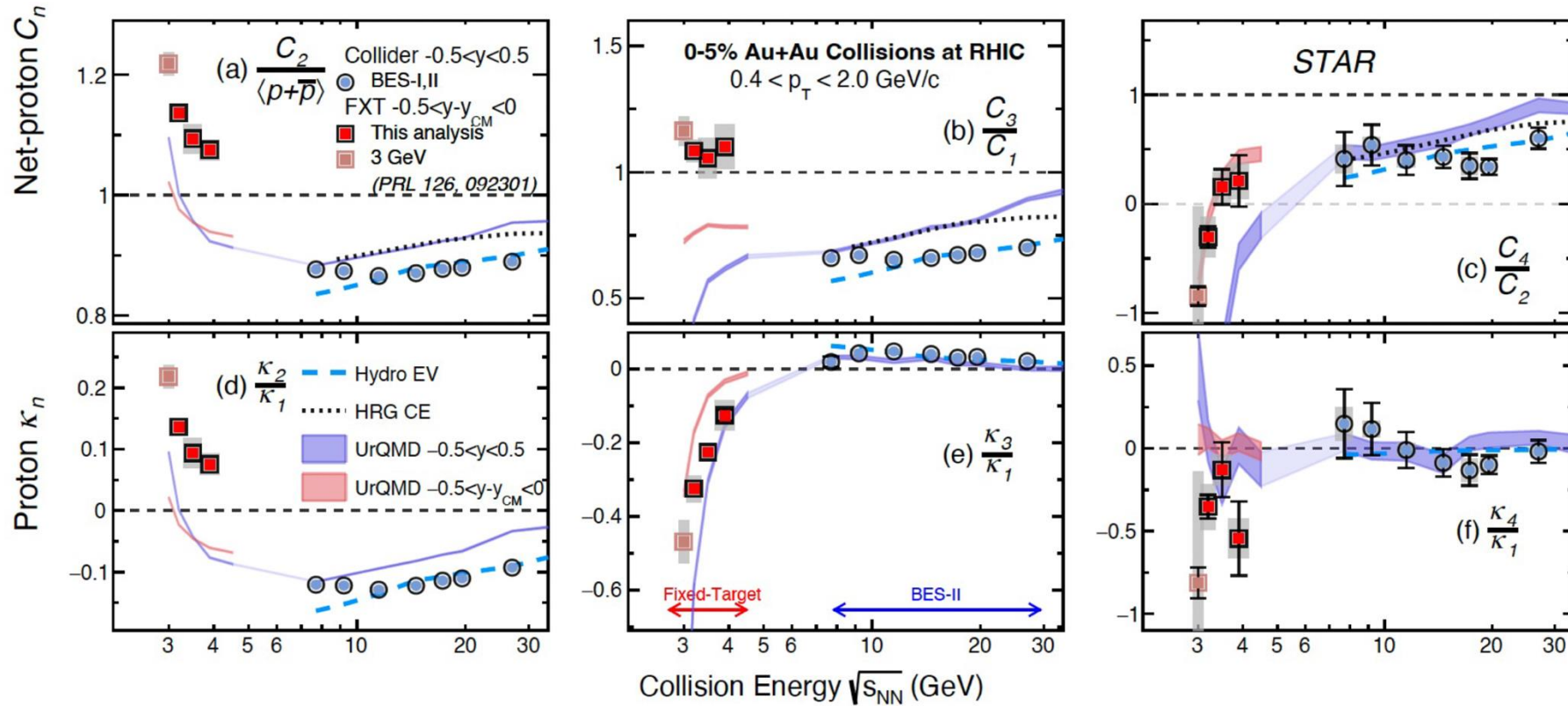
Precision results on net-proton
cumulants and proton factorial
cumulants from BES-II with greatly
improved statistical and systematic
uncertainties

Reduction factor in uncertainties on 0-5% C_4/C_2 :
BES-II vs BES-I

7.7 GeV		19.6 GeV	
stat. error	sys. error	stat. error	sys. error
4.7	3.2	4.5	4

2 - 5 σ deviation from peripheral data or
calculations without critical point effects

Net-proton cumulants and proton factorial cumulants from FXT energies



Proton C_4/C_2 , κ_4/κ_1 consistent with UrQMD

Proton (factorial) cumulants deviate from UrQMD at second and third order

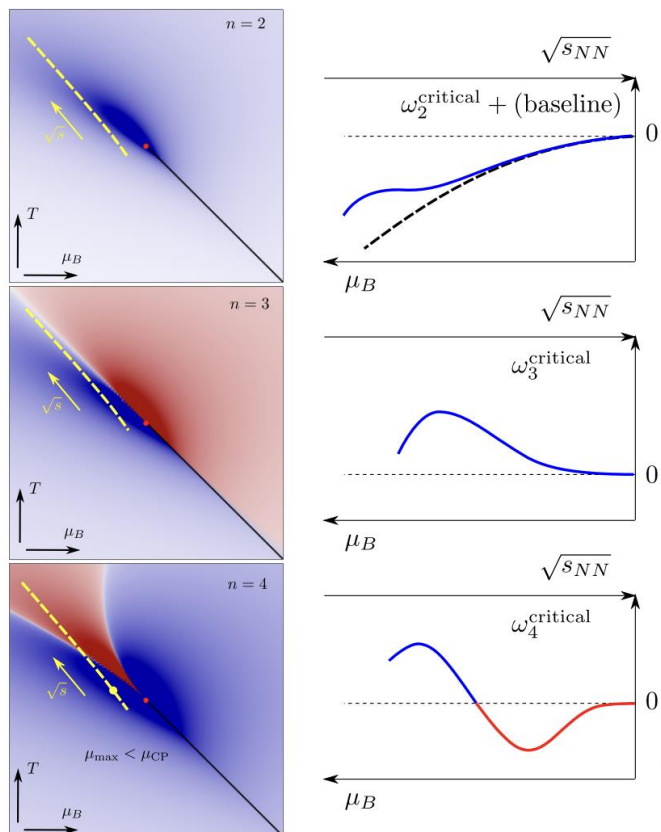
To do:

- Analyze 4.5 GeV and 2B 3 GeV data
- Study rapidity dependence

Proton and anti-proton factorial cumulants from 7.7 GeV to 27 GeV

arXiv: 2504.00817

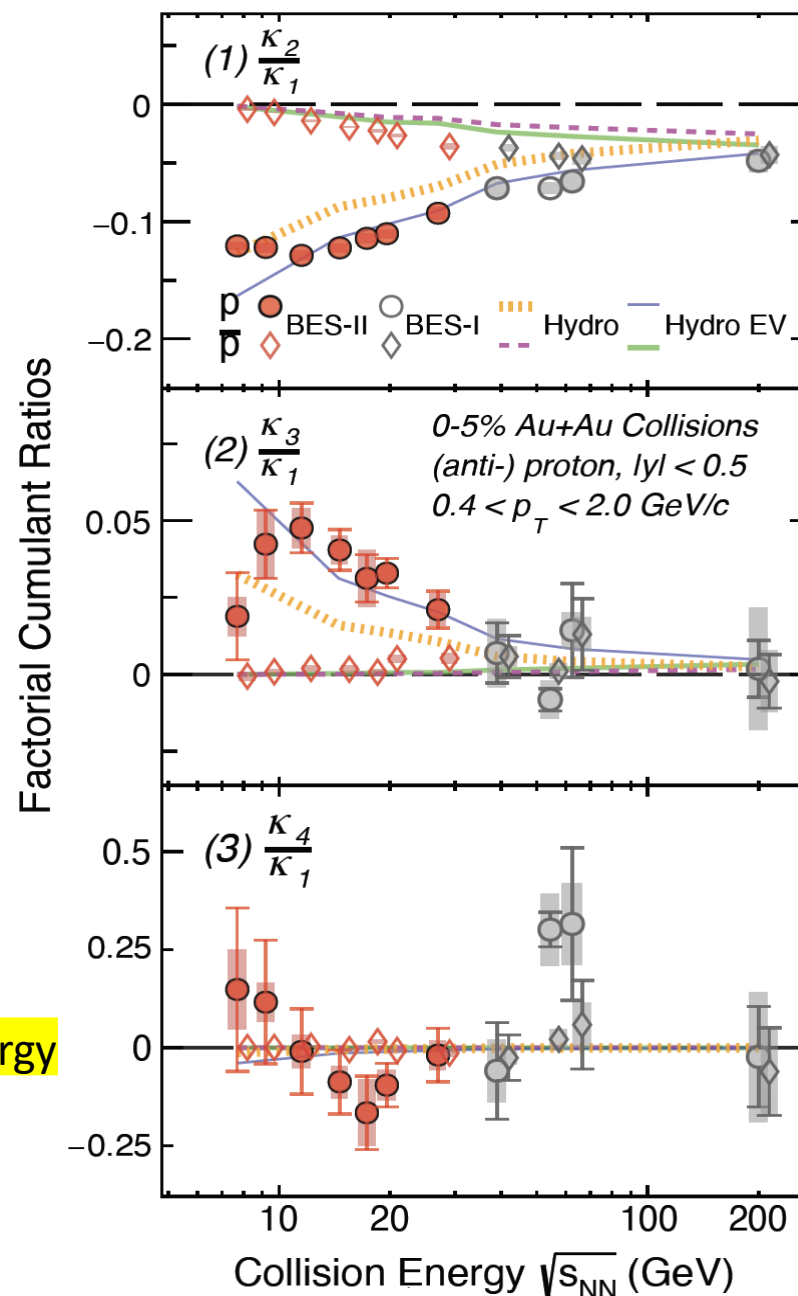
M. Stephanov, arXiv:2410.02861



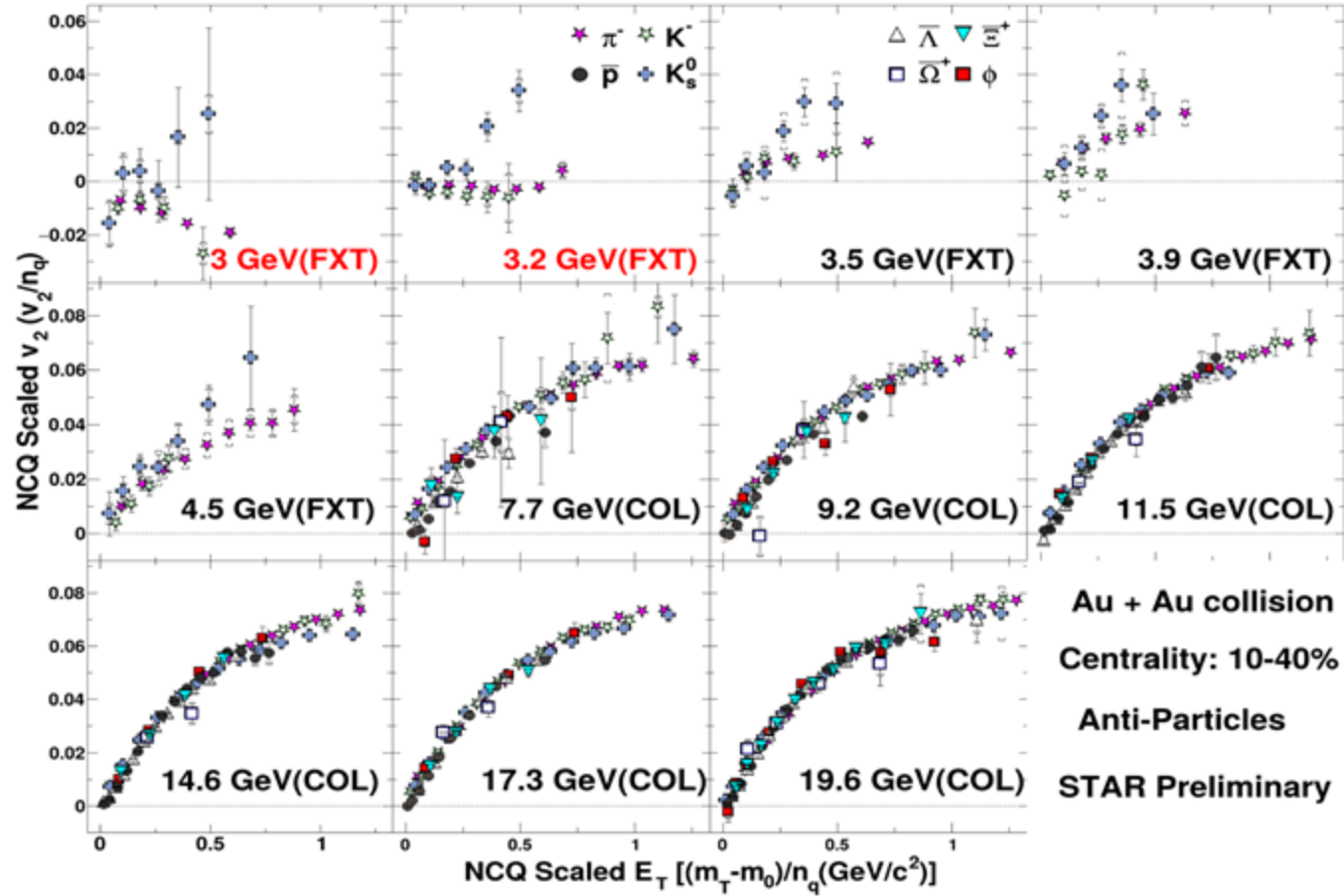
Very interesting trends observed as a function of collision energy

Critical needs:

- Baseline calculations without critical point effects
- Dynamic calculations with critical point effects

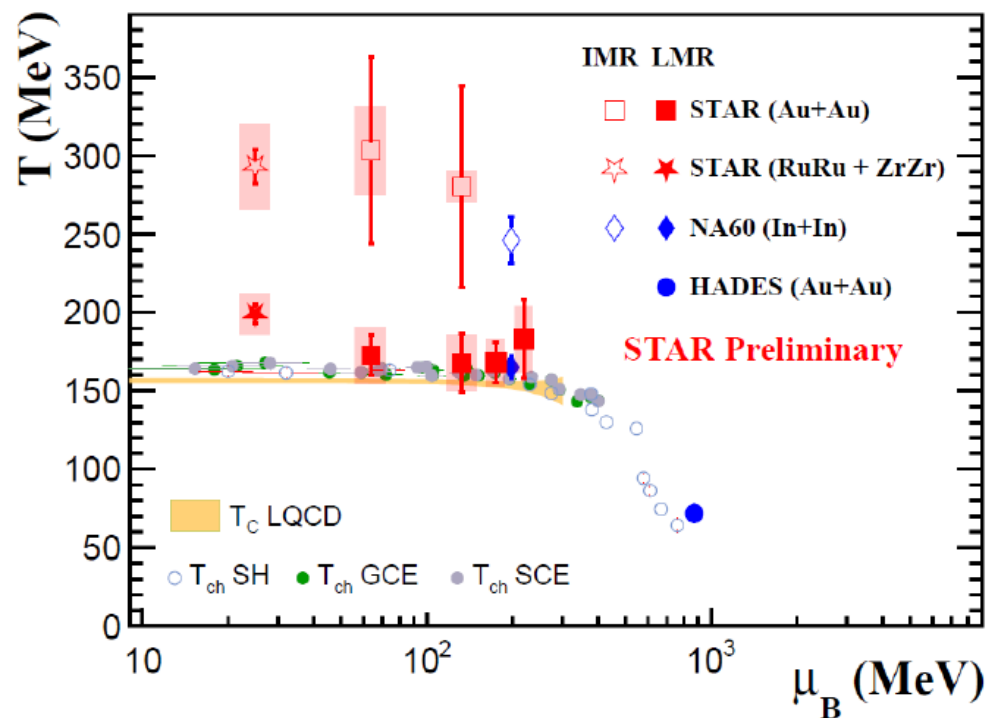
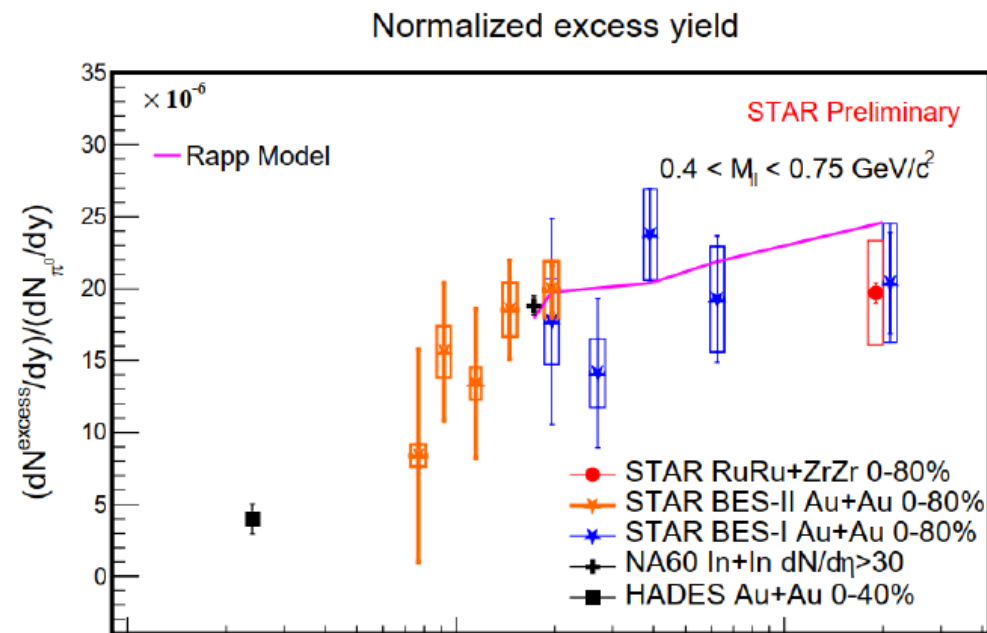
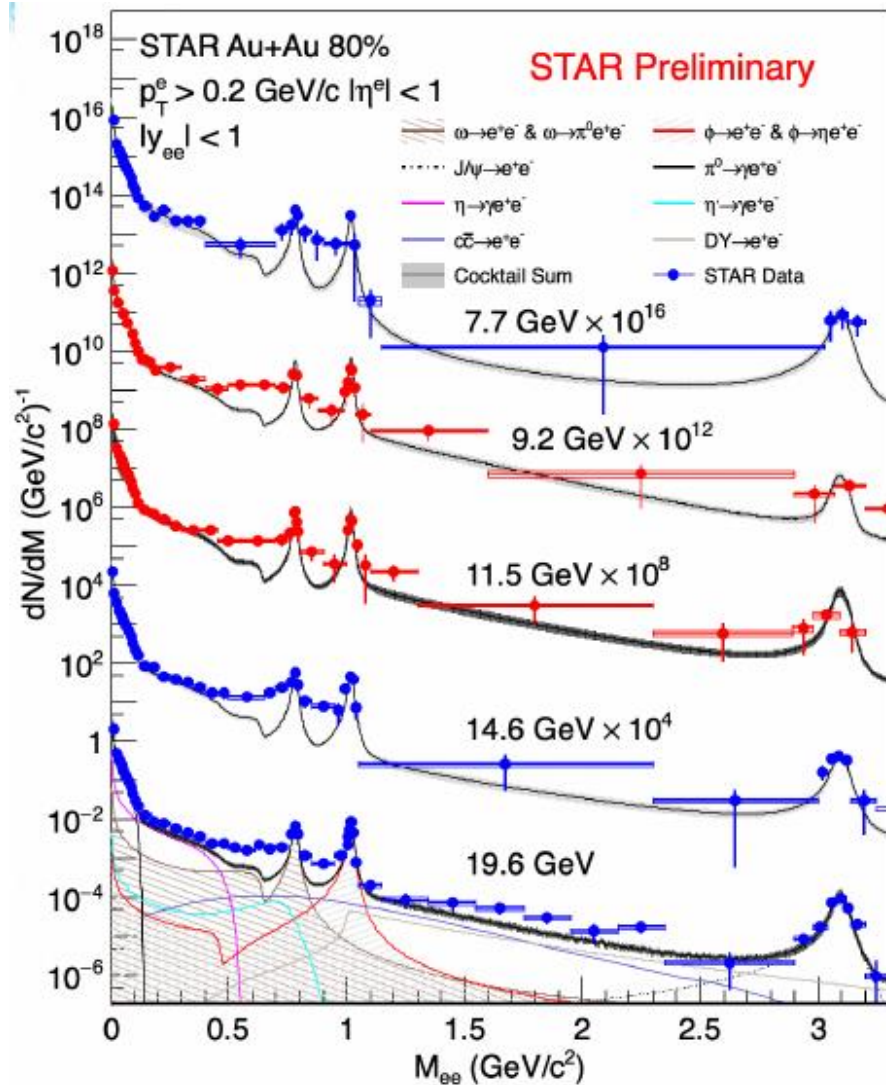


NCQ scaling of elliptic flow

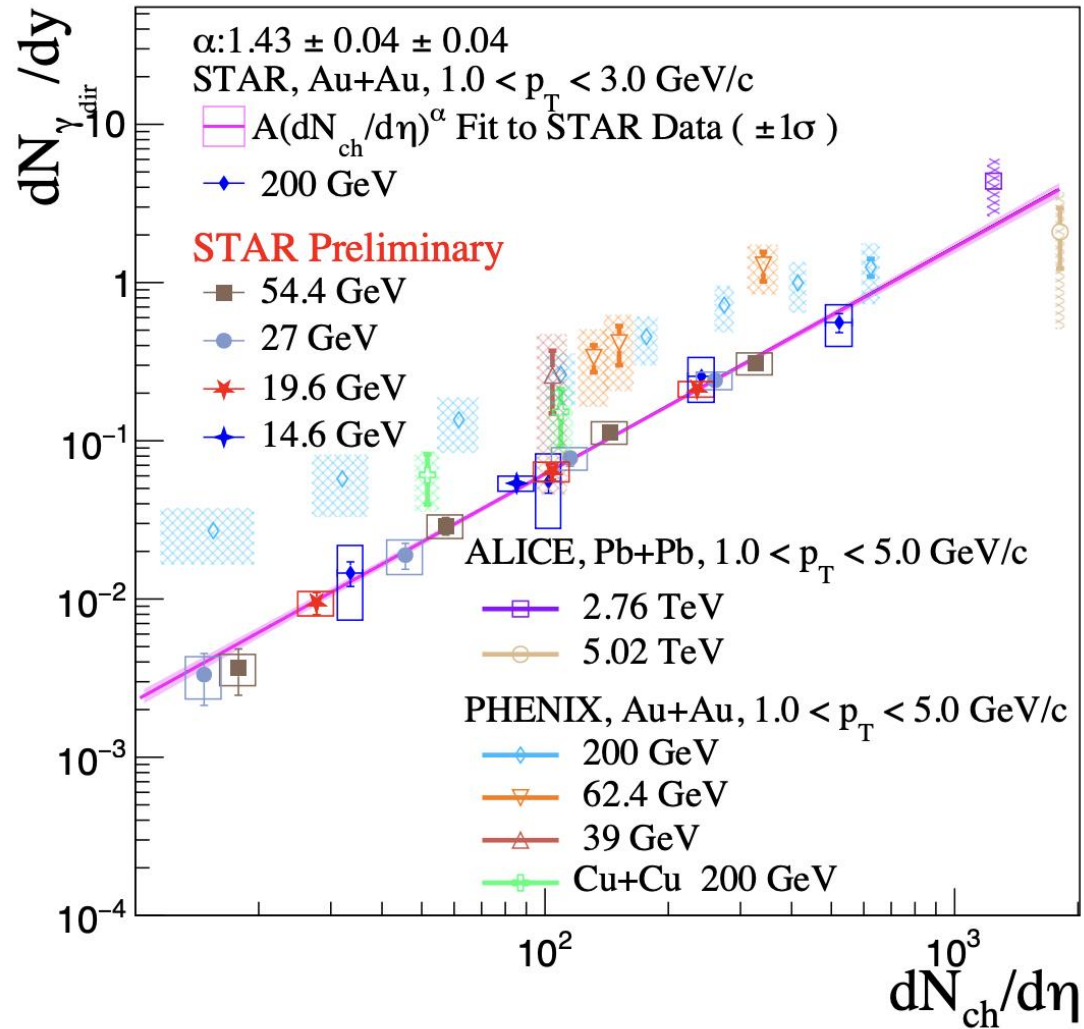


- NCQ scaling holds approximately for 7.7 GeV and above and completely breaks down at 3.2 GeV and below
- Constraints on nuclear shadowing and the onset of partonic collectivity

Thermal dileptons



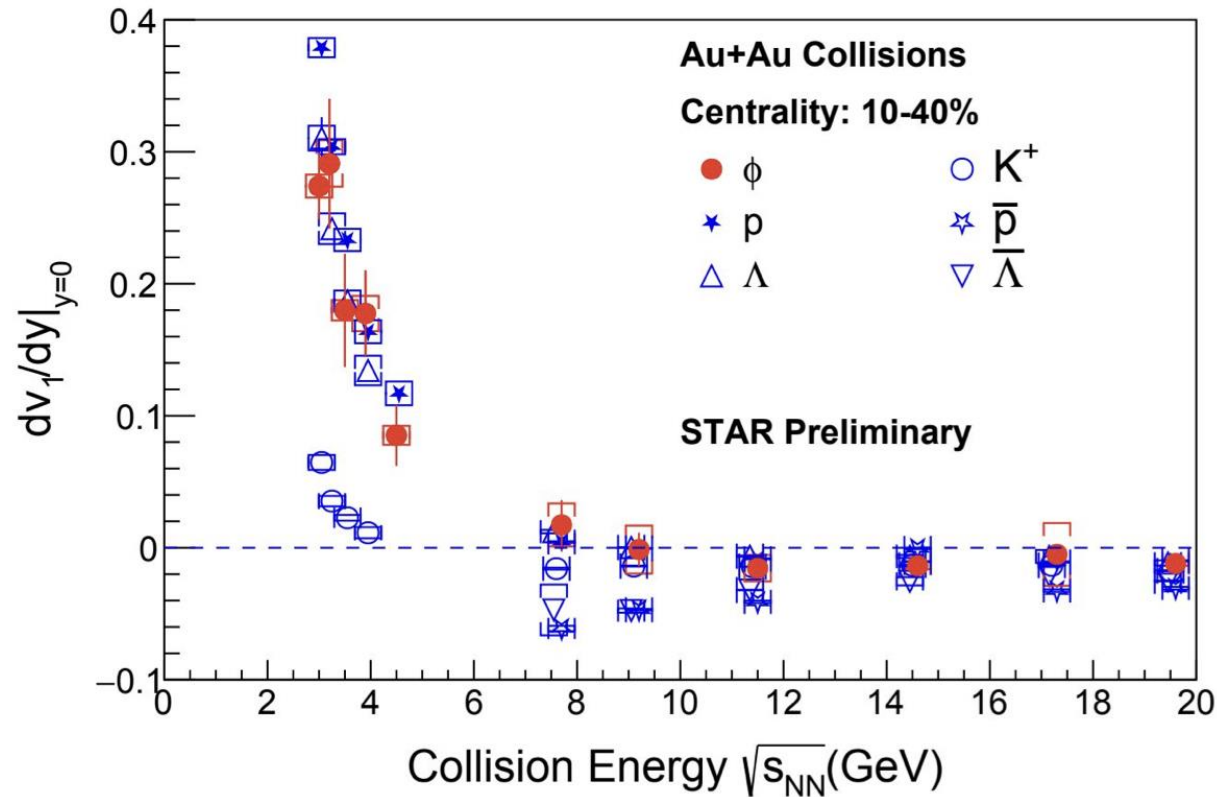
Direct virtual photons



- Yield of direct photons vs. multiplicity from 14.6 to 200 GeV

$$\alpha = 1.43 \pm 0.04 \pm 0.04$$

Directed flow of identified hadrons



Sensitive to the very early stages of the collision

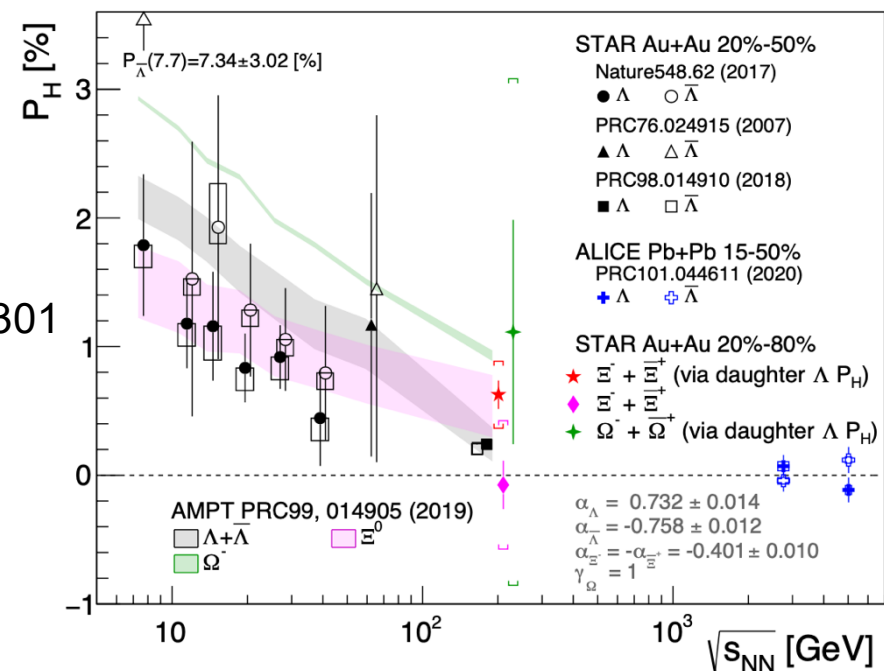
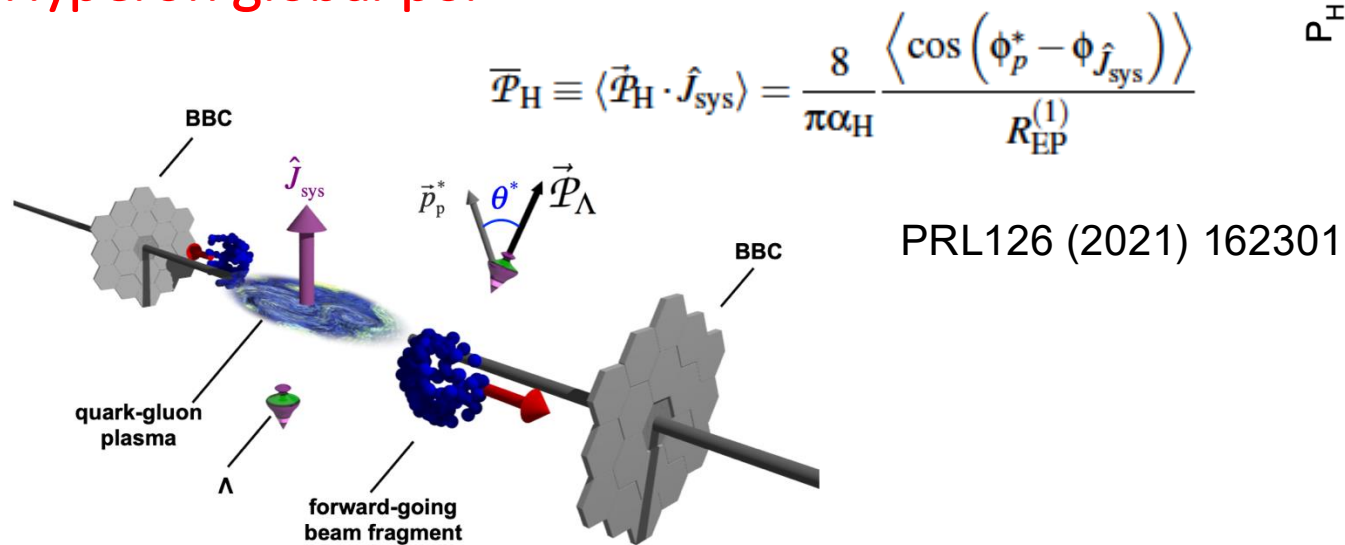
v_1 slope:

- ϕ meson behavior is similar to protons and lambdas
- Matches kaons at 9.2 GeV and above, but shows significant deviations in the FXT energy region

What is the underlying physics mechanism?

Momentum-dependent mean field potential at lower energies?

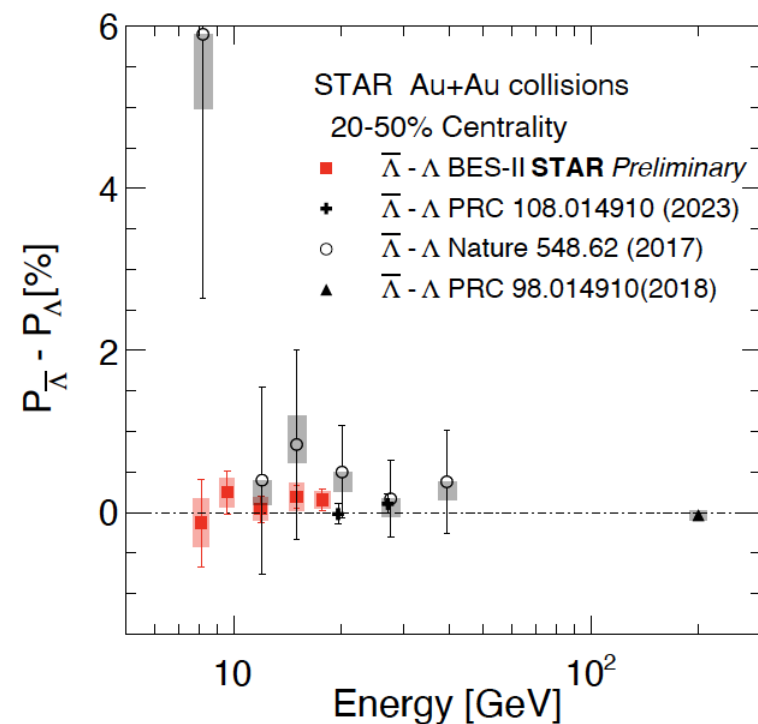
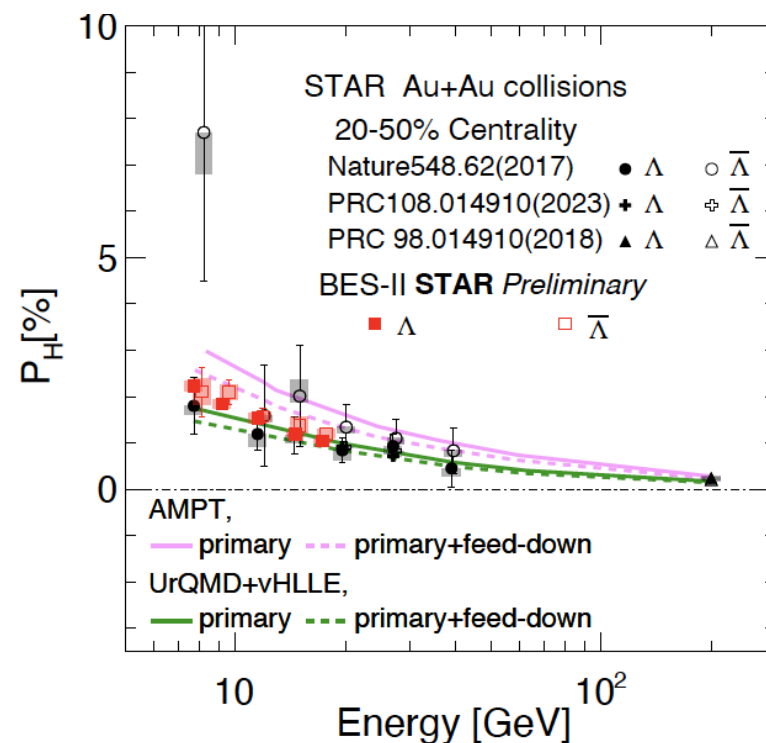
Hyperon global polarization



Global angular momentum transfer to hyperon polarization

Heavy ion collisions created the most vortical system ever observed.

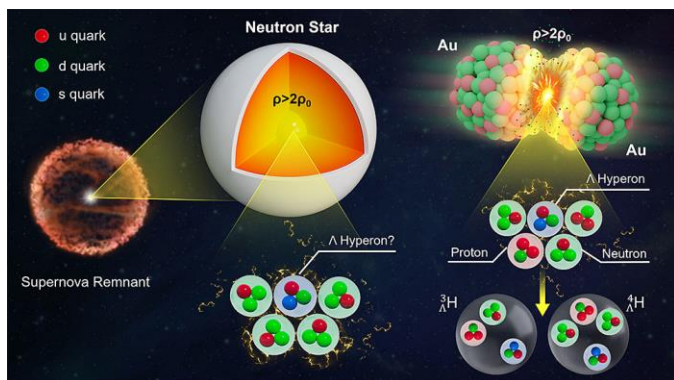
Nature **548** (2017) 62



$$(P_{\bar{\Lambda}} - P_{\Lambda}) \approx \frac{2|\mu_{\Lambda}|B}{T}$$

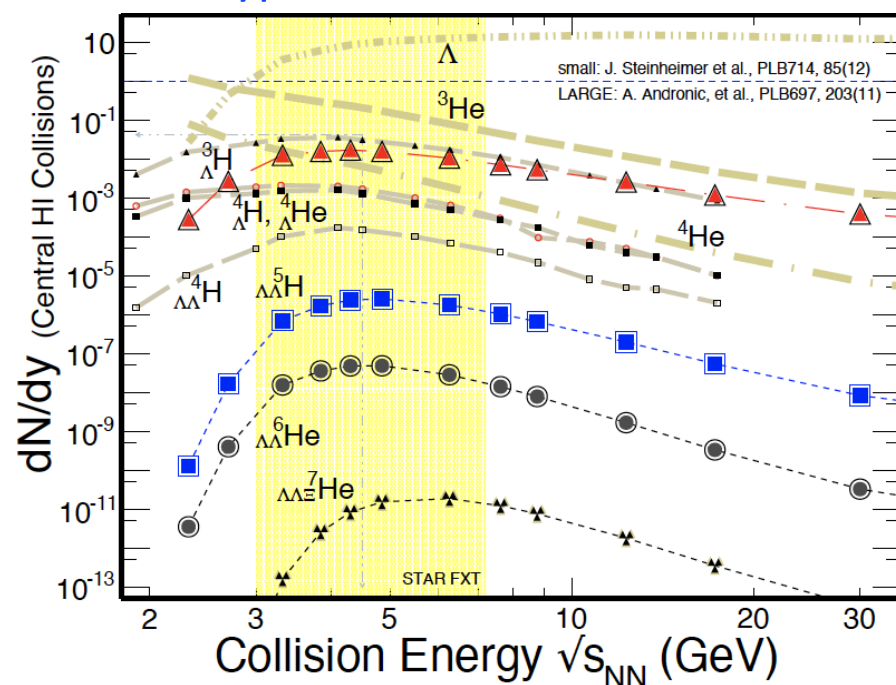
$T = 150 \text{ MeV}$
 $\mu_{\Lambda} = -1.93 \times 10^{-14} \text{ MeV/T}$

Hypernuclei production

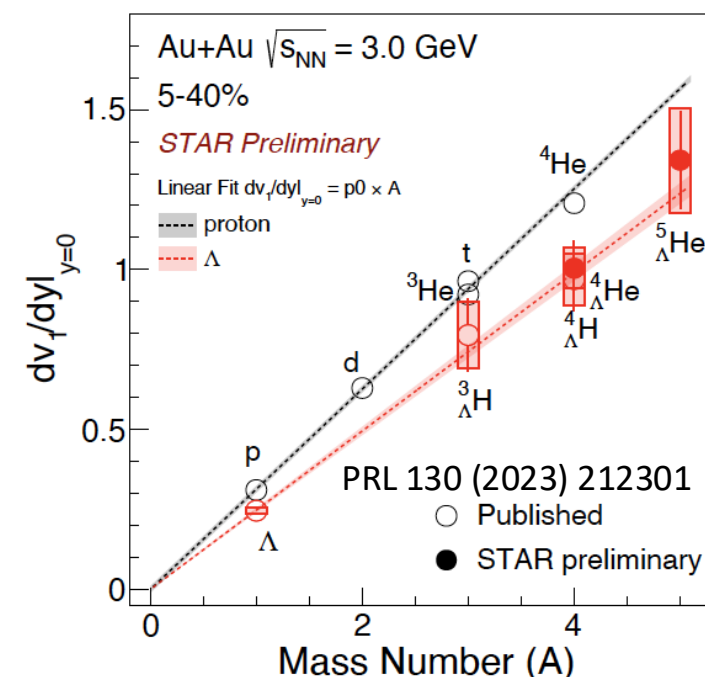
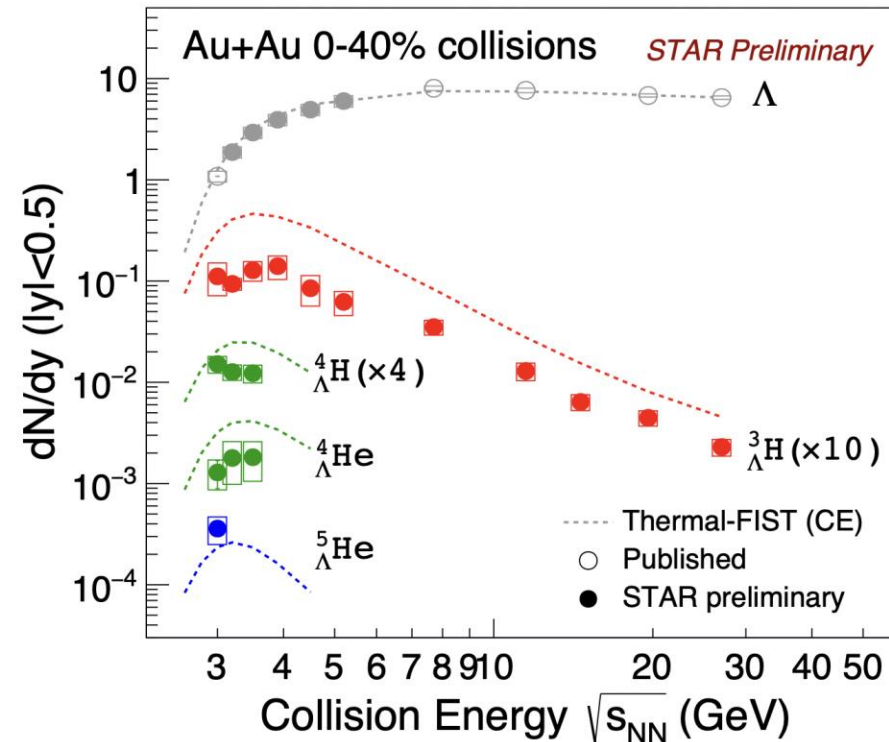


Picture credit:
BNL news article
<https://www.bnl.gov/newsroom/news.php?p?a=121192>

Hypernuclei Production



Constrain hyperon – nucleon and hyperon-hyperon interaction
Connection to neutron stars



Midrapidity v_1 slopes follow baryon number scaling, implying that coalescence is the dominant production mechanism

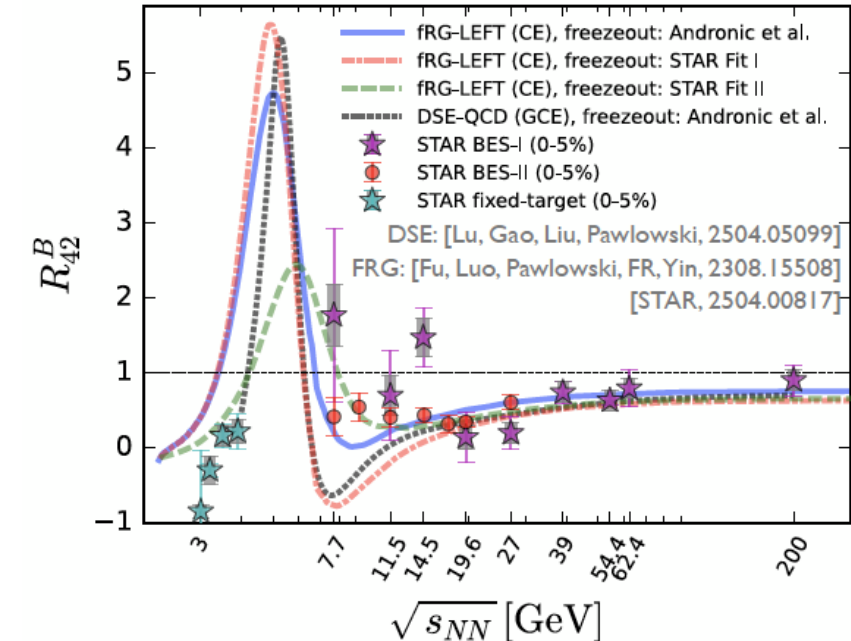
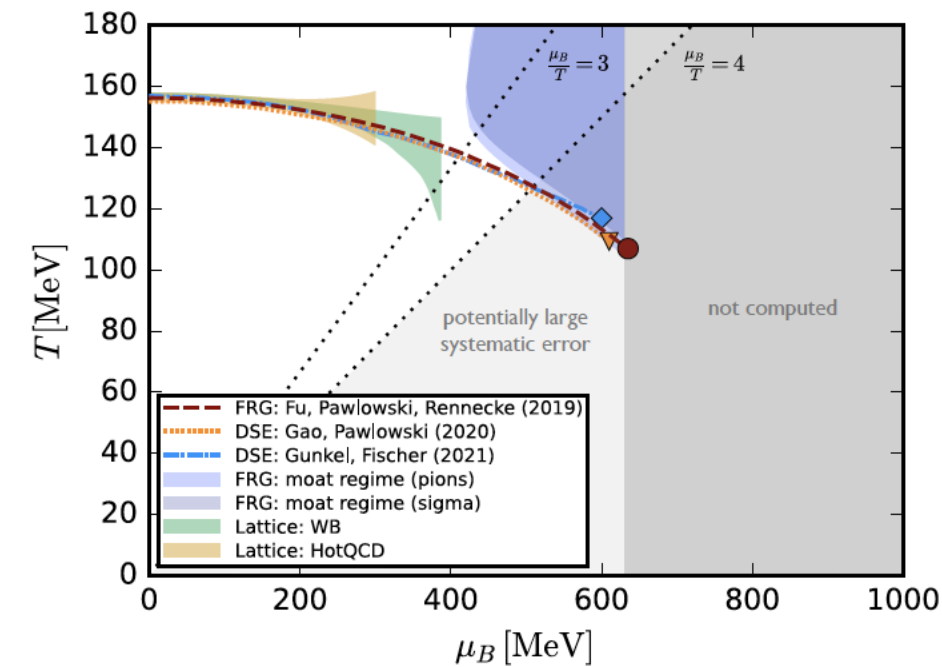
Summary: beam energy scan program

The RHIC BES program has been highly successful, thanks to strong community support and many years of dedicated planning and preparation.

The BES data cover a broad and interesting range of μ_B , enabling us to:

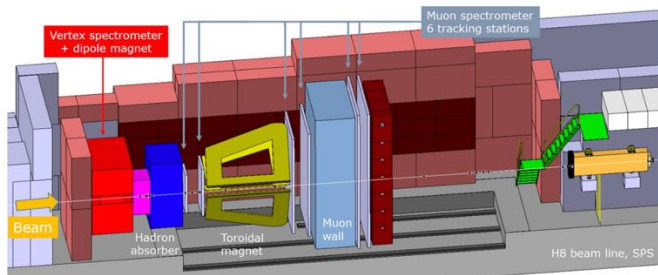
- Search for the QCD critical point
- Explore signatures of a first-order phase transition
- Investigate the onset of QGP formation
- Study hyperon-nucleon interactions
- Examine the vorticity field in heavy-ion collisions
- Measure the freeze-out properties
- ...

Stay tuned—many more exciting results are on the way!

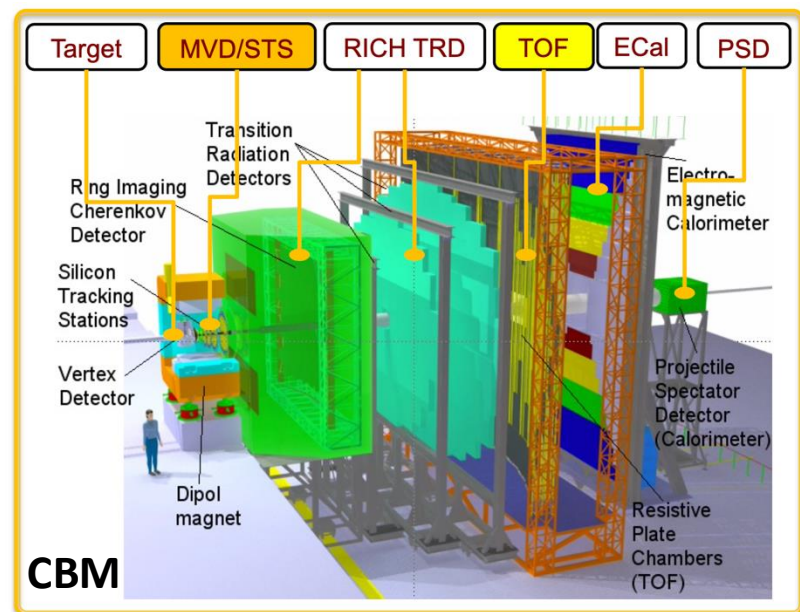
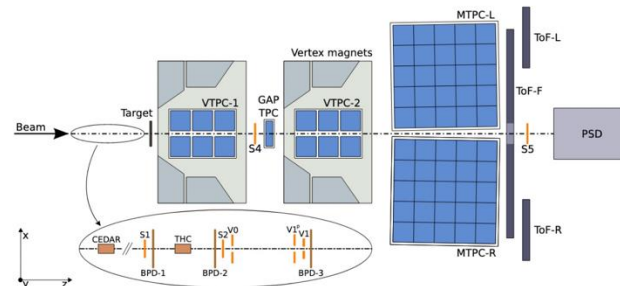


The future

NA60⁺ (2029)

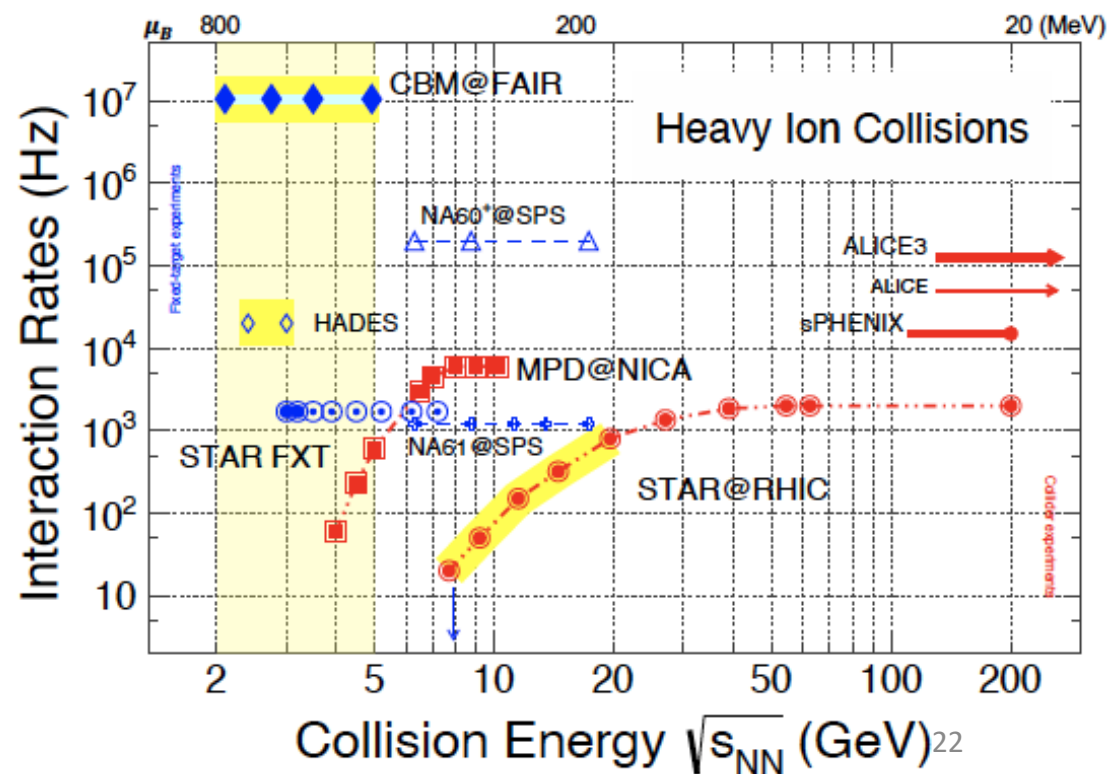


NA61 (2008 - 2027)



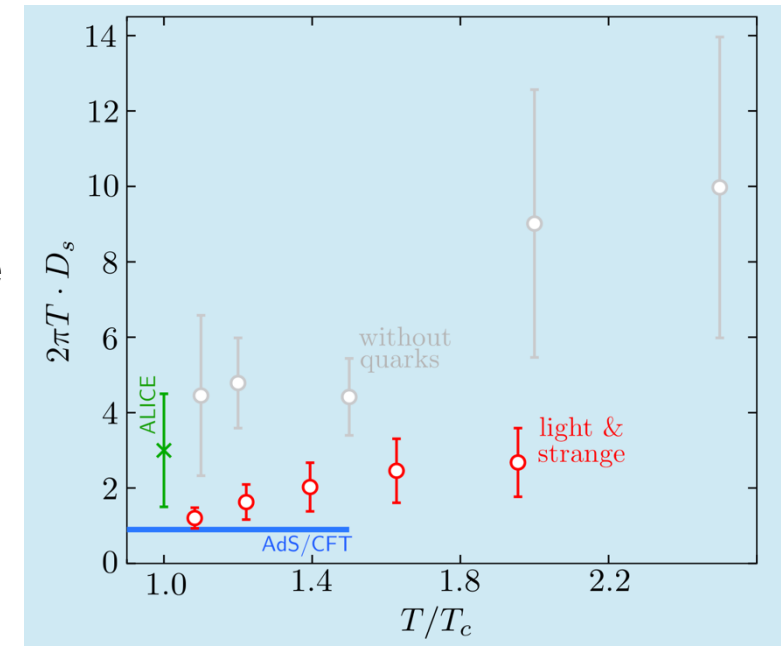
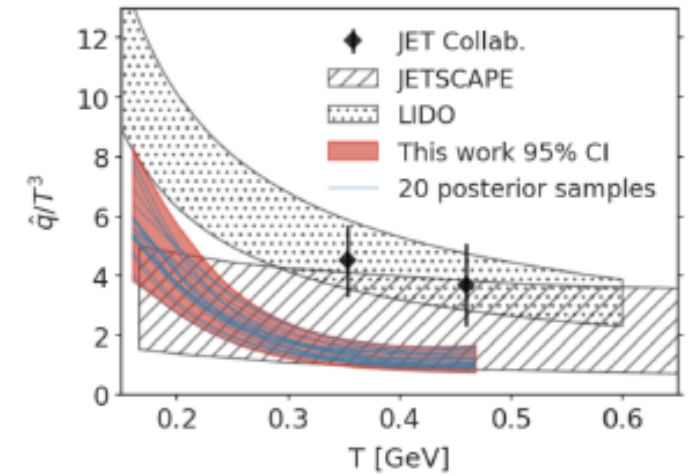
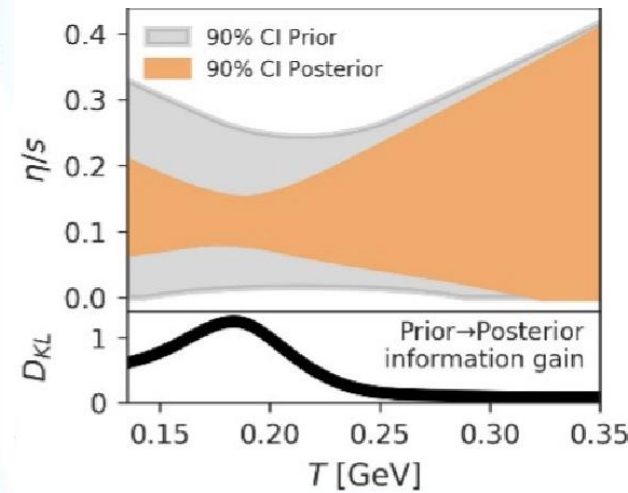
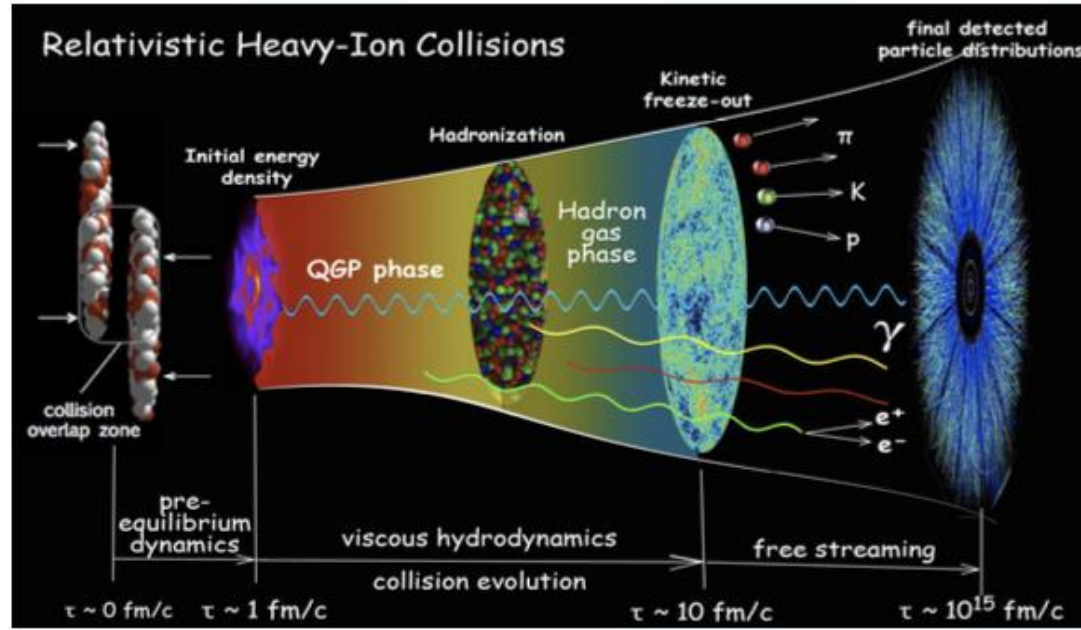
Physics opportunities in the exploration of the QCD phase diagram at high baryon density after the completion of the RHIC BES-II program: NA60+, NA61, CBM, NICA ...

Probe the physics of dense baryon-rich matter and constrain the nuclear equation of state in a regime relevant to binary neutron star mergers and supernovae.



The properties of perfect liquid

The 2023 NSAC Long Range Plan for Nuclear Science



Essential questions to be addressed:

1. How do the fundamental interactions between quarks and gluons lead to the perfect fluid behavior of the quark-gluon plasma?
2. What are the limits on the fluid behavior of matter?
3. What are the properties of QCD matter?
4. What is the nature of the transition from QGP to hadronic matter?
5. Does a QCD critical point exist, analogous to the critical point in the water–vapor–ice phase diagram?

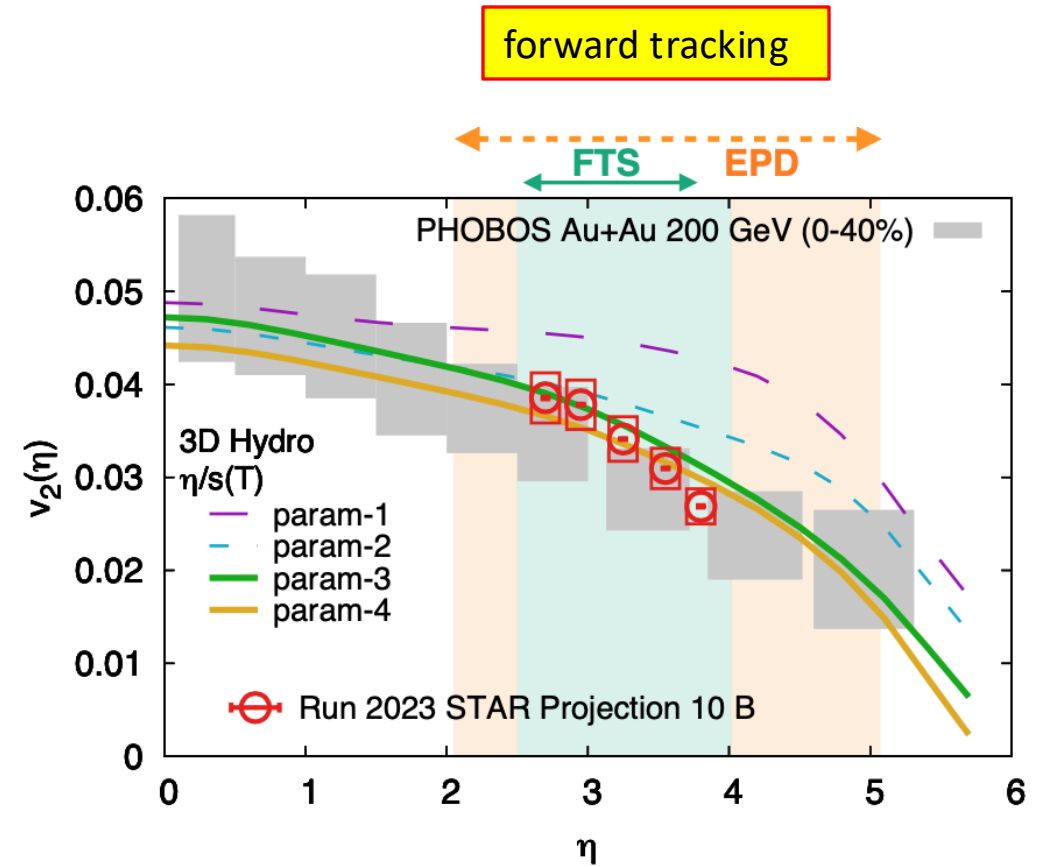
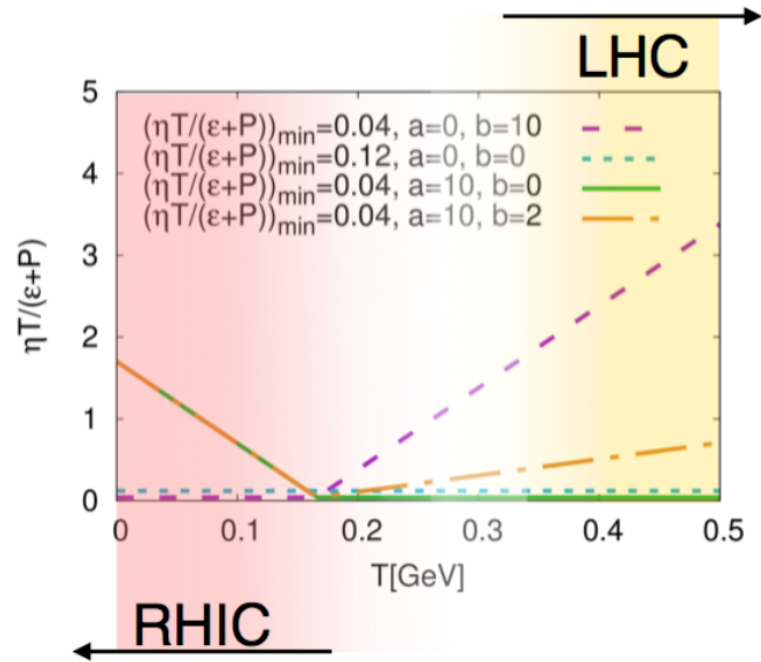
To address important questions about the inner workings of the QGP

- What is the nature of the 3-dimensional initial state at RHIC energies? r_n over a wide rapidity, J/ψ v_1 , photon Wigner distributions
- What is the precise temperature dependence of shear and bulk viscosity? v_n as a function of η
- What can be learned about confinement from charmonium measurements? J/ψ v_2
- What is the temperature of the medium? Different Υ states, $\psi(2S)$, thermal dileptons
- What are the electrical, magnetic, and chiral properties of the medium? Λ , Ξ , Ω P_H and K^* , ϕ , J/ψ ρ_{00} , thermal dileptons, CME observables
- What are the underlying mechanisms of jet quenching at RHIC energies? What do jet probes tell us about the microscopic structure of the QGP as a function of resolution scale? $\gamma_{dir}+jet$ I_{AA} , $\gamma_{dir}+jet$ acoplanarity, jet substructure
- What is the precise nature of the transition near $\mu_B=0$? Net-proton C_6/C_2
- What can we learn about the strong interaction? Correlation functions

To inform EIC physics with photon induced processes:

- Probe gluon distribution inside the nucleus: vector mesons (J/ψ), dijets (?)
- Search for collectivity and signatures of baryon junction: inclusive charge particles and cross sections, v_n , identified particle spectra

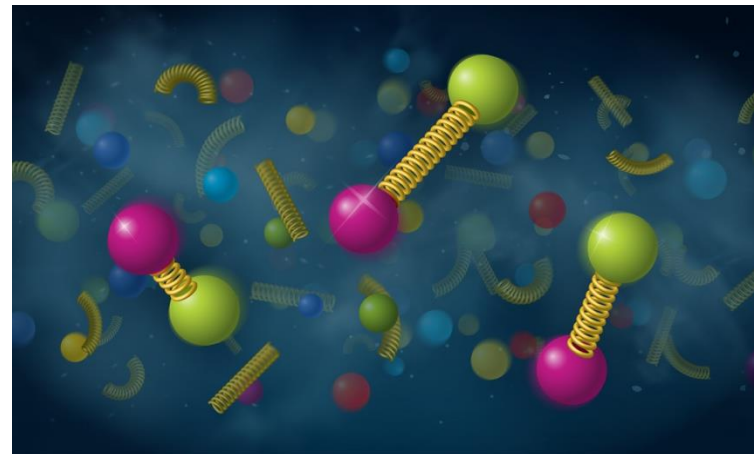
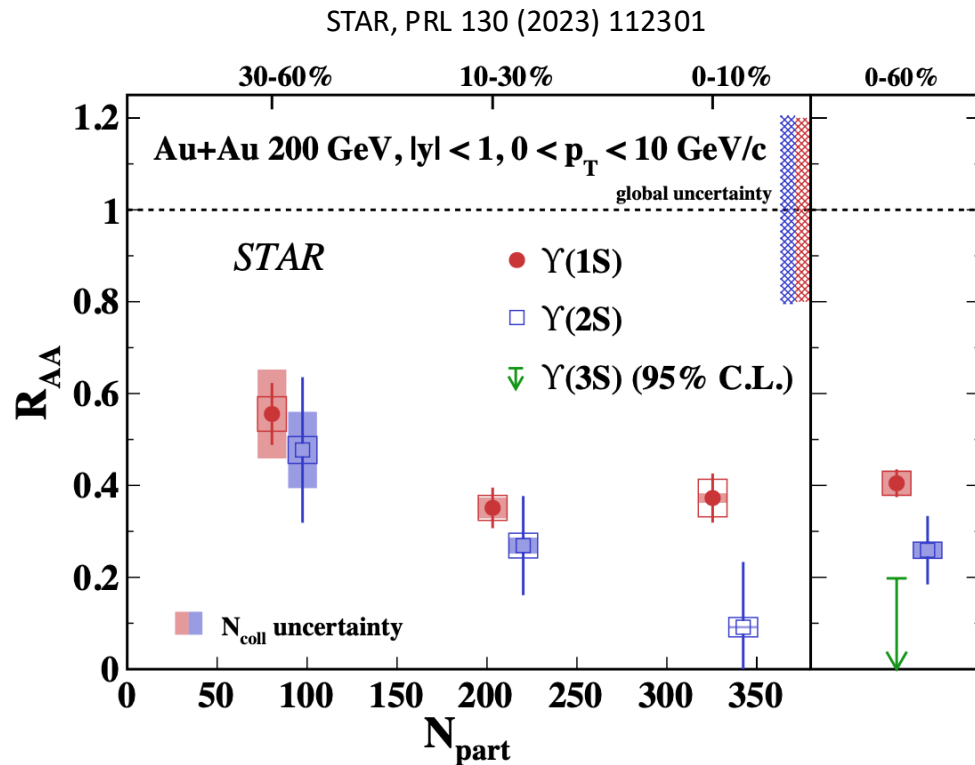
Constrain temperature dependence of η/s



Flow measurements at forward rapidity sensitive to η/s as a function of T .

Much more precise than previous PHOBOS measurements.

Sequential Upsilon suppression



$\Upsilon(1S)$, $\Upsilon(2S)$, $\Upsilon(3S)$ sizes: 0.28, 0.56, 0.78 fm

Negligible contribution from b and \bar{b} recombination at RHIC

$$\Upsilon(1S) R_{AA} = 0.40 \pm 0.03 \text{ (stat.)} \pm 0.03 \text{ (sys.)} \pm 0.07 \text{ (norm.)}$$

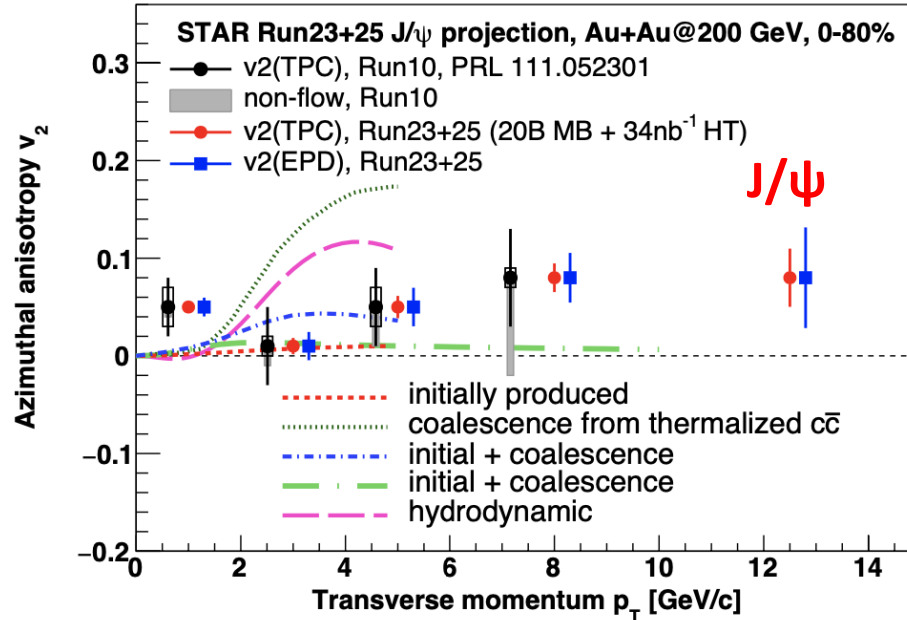
$$\Upsilon(2S) R_{AA} = 0.26 \pm 0.07 \text{ (stat.)} \pm 0.02 \text{ (sys.)} \pm 0.04 \text{ (norm.)}$$

$$\Upsilon(3S) R_{AA} \text{ upper limit: } 0.20 \text{ at a 95\% confidence level}$$

Sequential Υ suppression at RHIC

Deconfinement and thermalization

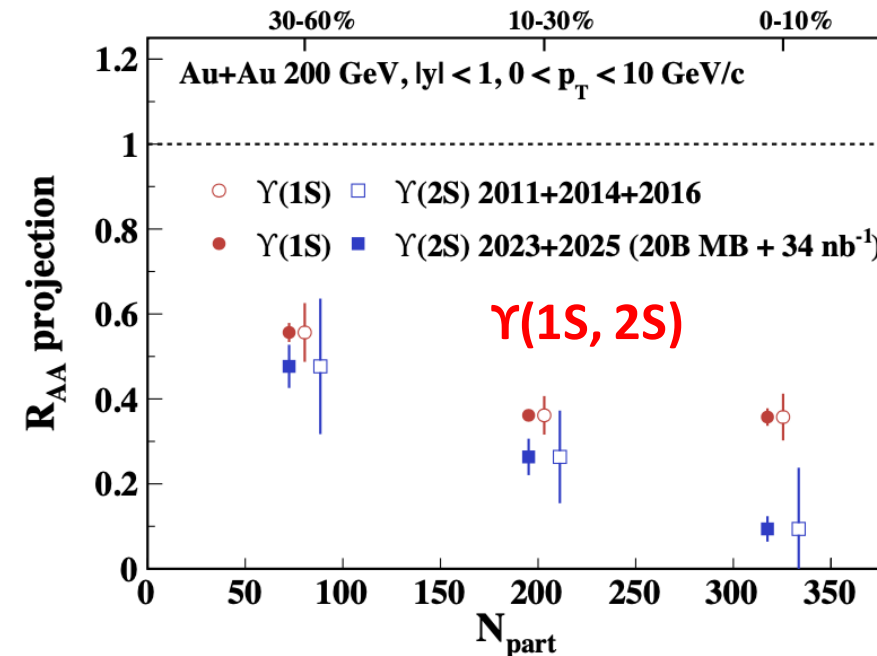
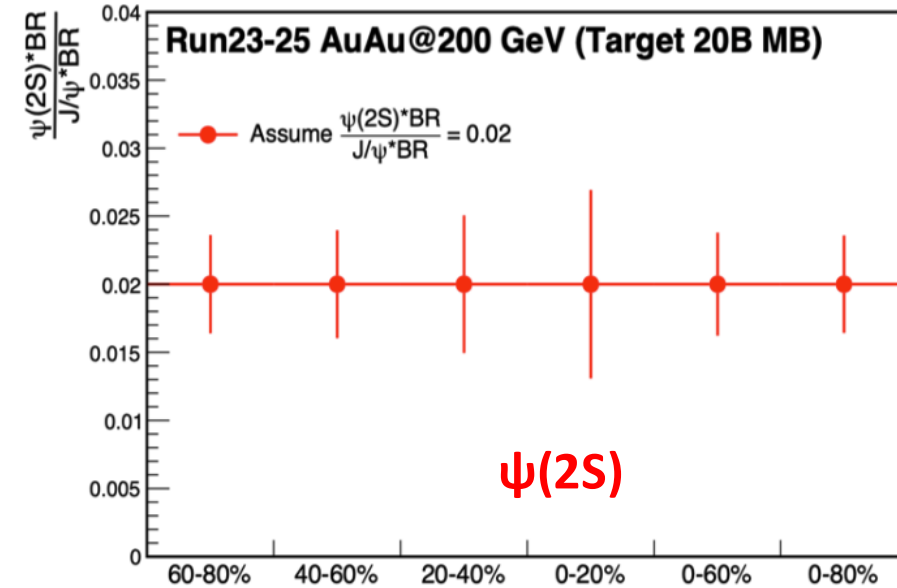
low material, improved PID, extended η coverage by iTPC



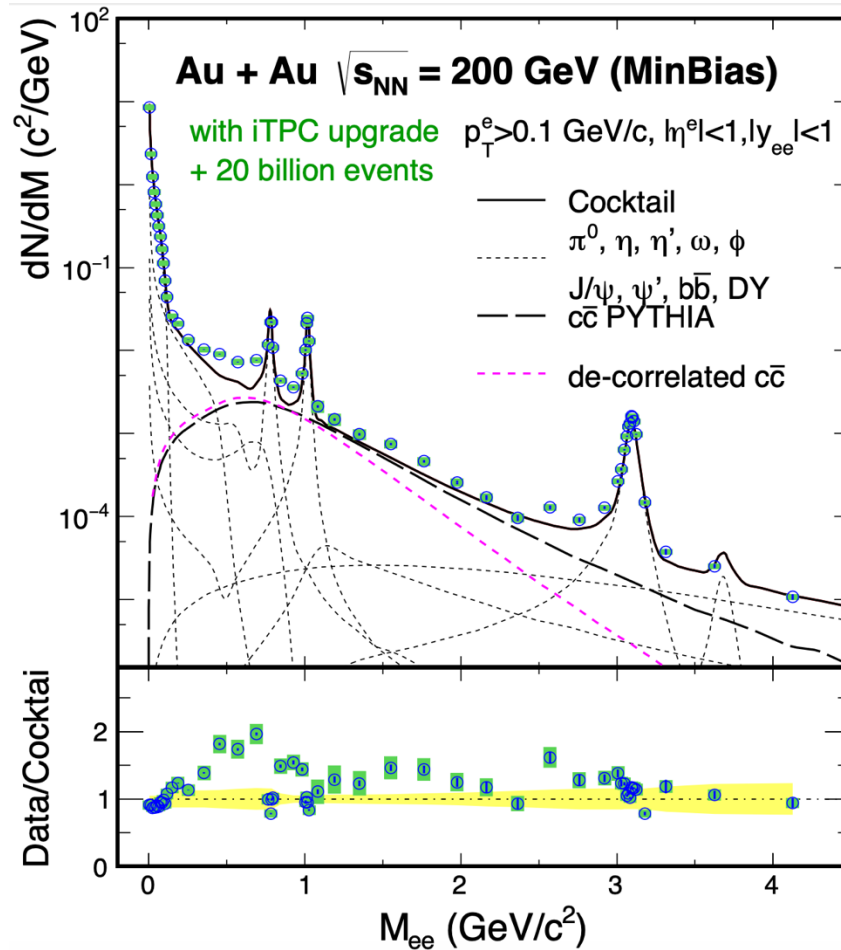
J/ψ: interplay of color-screening, gluon dissociation, and recombination, signature of deconfinement

- low p_T v_2 : recombination

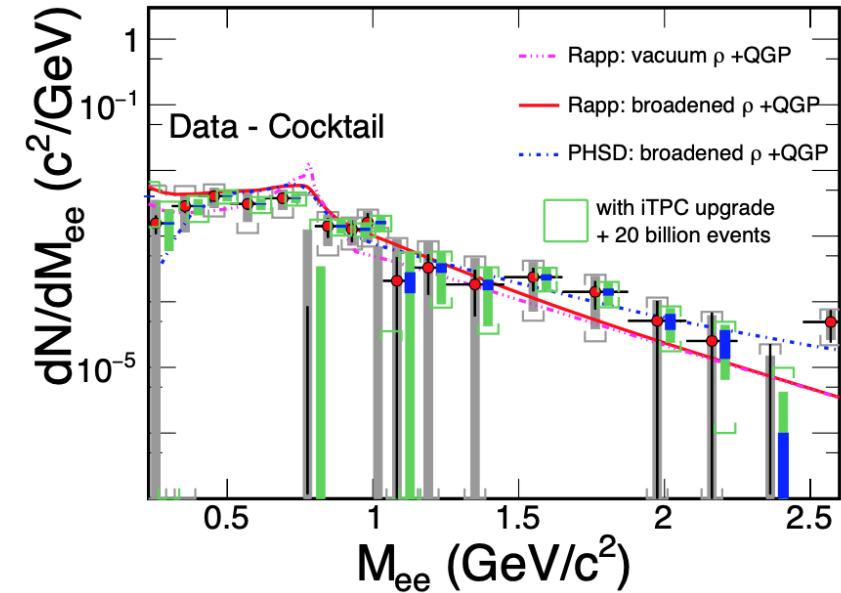
Explore temperature profile of the medium: $\psi(2S)$ suppression, different Υ states, thermal dileptons



Chiral property



low material, improved PID, extended η and p_T coverage by iTPC



Low-mass dielectron measurement: **lifetime indicator** and provide a stringent constraint for theorists to establish chiral symmetry restoration at $\mu_B \sim 0$

Intermediate mass: **direct thermometer** to measure temperature

Enable dielectron v_2 and polarization, and solve direct photon puzzle (STAR vs PHENIX)

Charge dependent directed flow

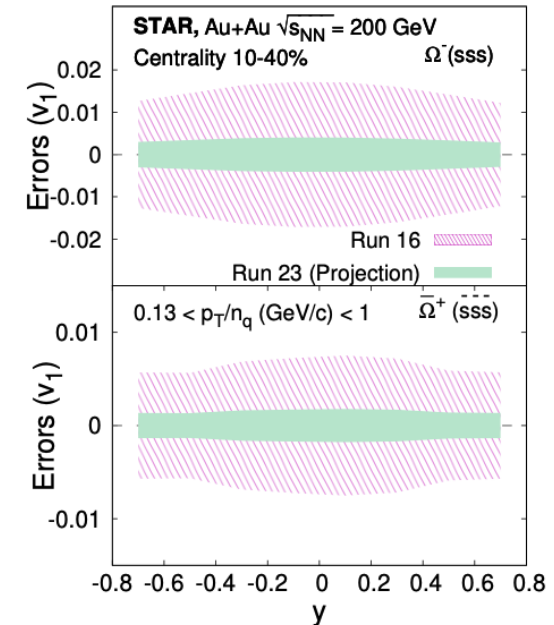
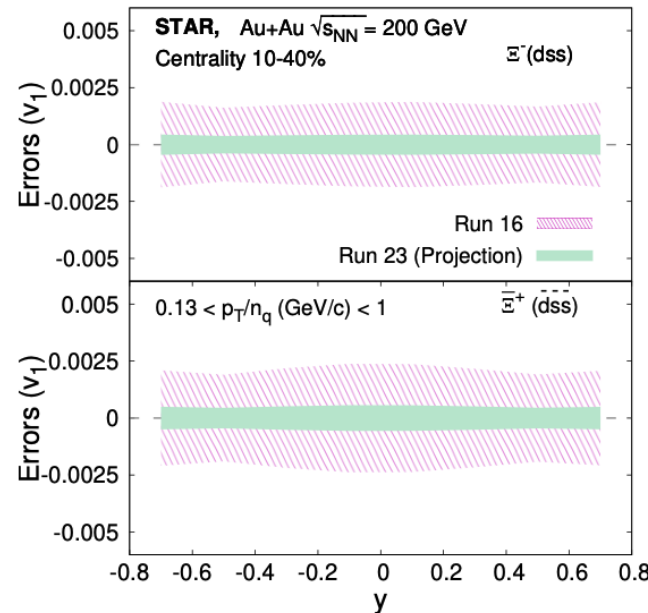
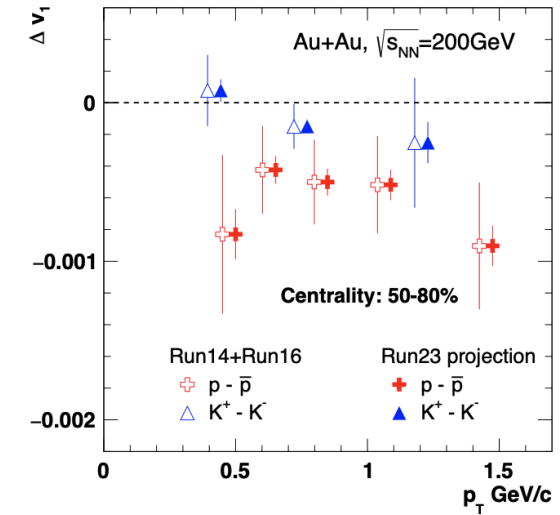
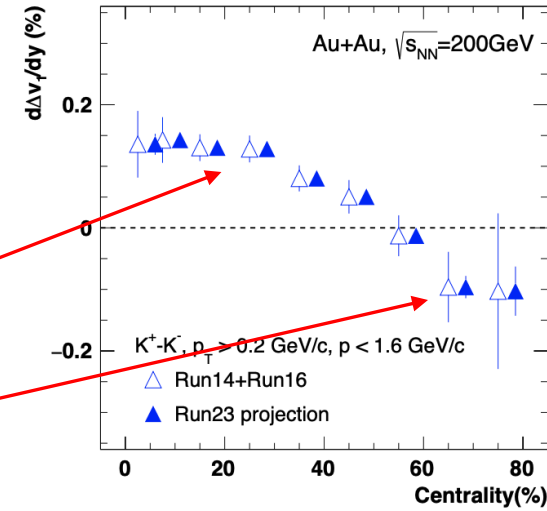
improved PID, extended η coverage by iTPC

Charge dependent v_1 slope sensitive to EM field

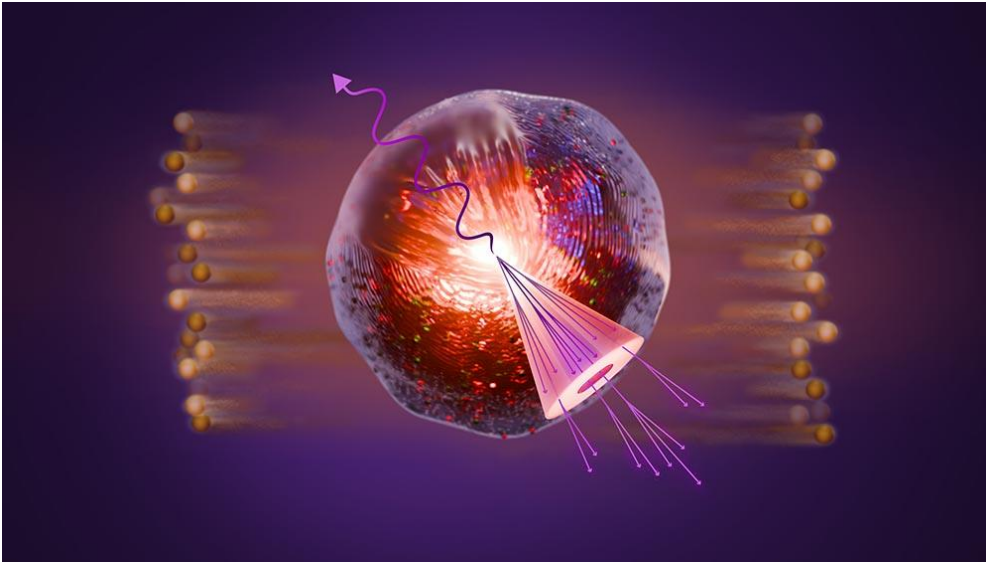
$d\Delta v_1/dy > 0$ due to transported quark

$d\Delta v_1/dy < 0$ due to EM field

Runs 23+24+25: $>5\sigma$ difference between K^+ and K^- in peripheral collisions, precise measurements for multi-strange particles.



Jet quenching observables



<https://www.bnl.gov/newsroom/news.php?a=122311>

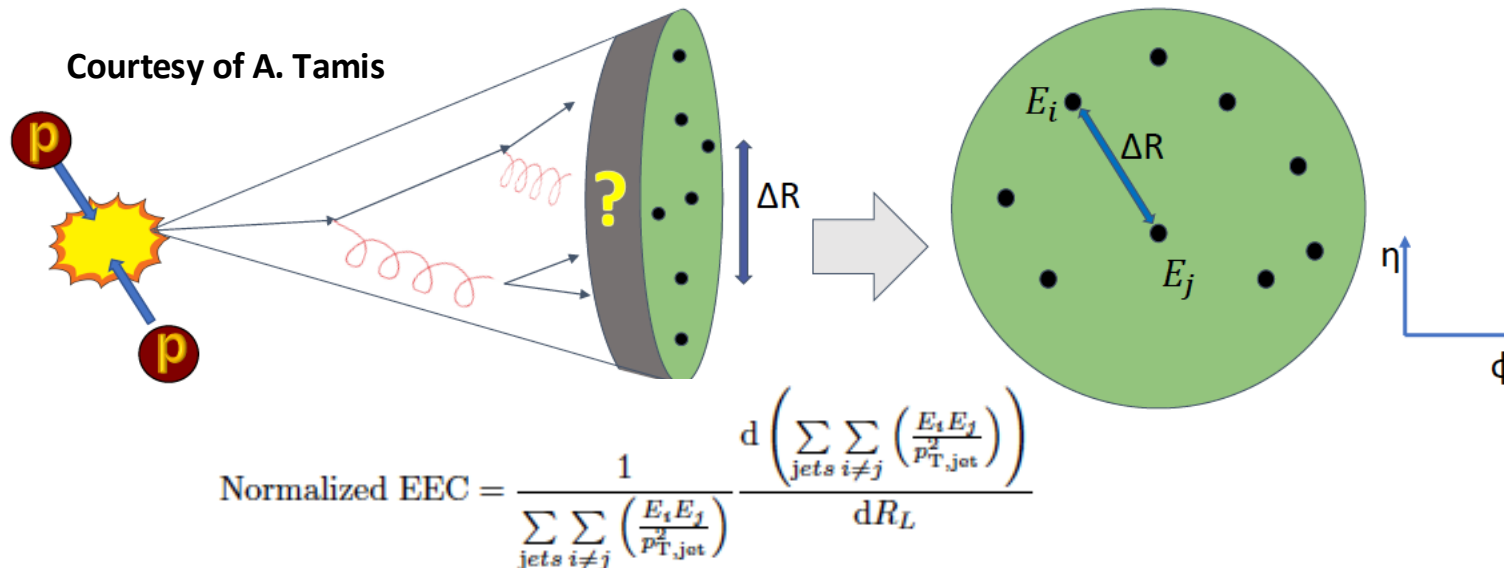
Trigger-normalized semi-inclusive recoil-jet distribution

$$\frac{1}{N_{\text{trig}}} \frac{dN_{\text{jet}}}{dp_{T,\text{jet}}^{\text{ch}}} \bigg|_{p_T^{\text{trig}}}$$

I_{AA} = measurement in Au+Au / measurement in p+p

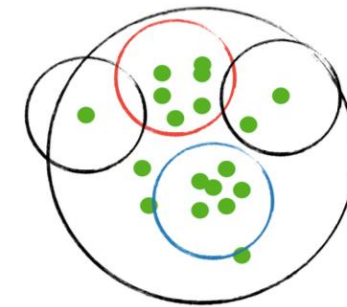
γ_{dir} + jet acoplanarity: azimuthal angle difference between the recoiled jet and the gamma jet

Energy-energy correlator: how energy is distributed as a function of the separation



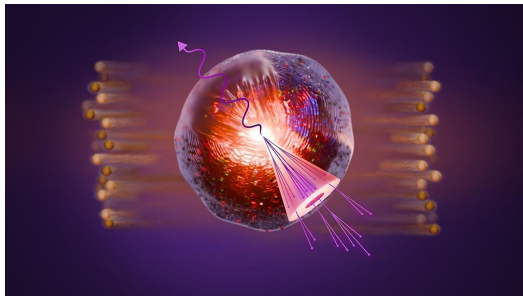
R_L : angular separation between two distinct tracks within a jet

Jet substructure



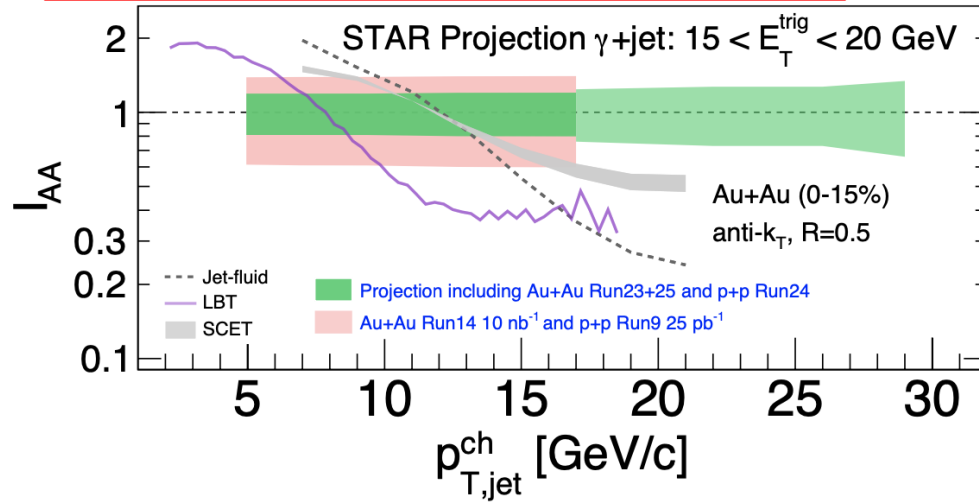
Red: leading sub-jet
Blue: sub-leading sub-jet
 $Z_{\text{SJ}} = p_T^{\text{blue}} / (p_T^{\text{blue}} + p_T^{\text{red}})$
 $\theta_{\text{SJ}} = \Delta R(\text{blue}, \text{red})$

Jet quenching

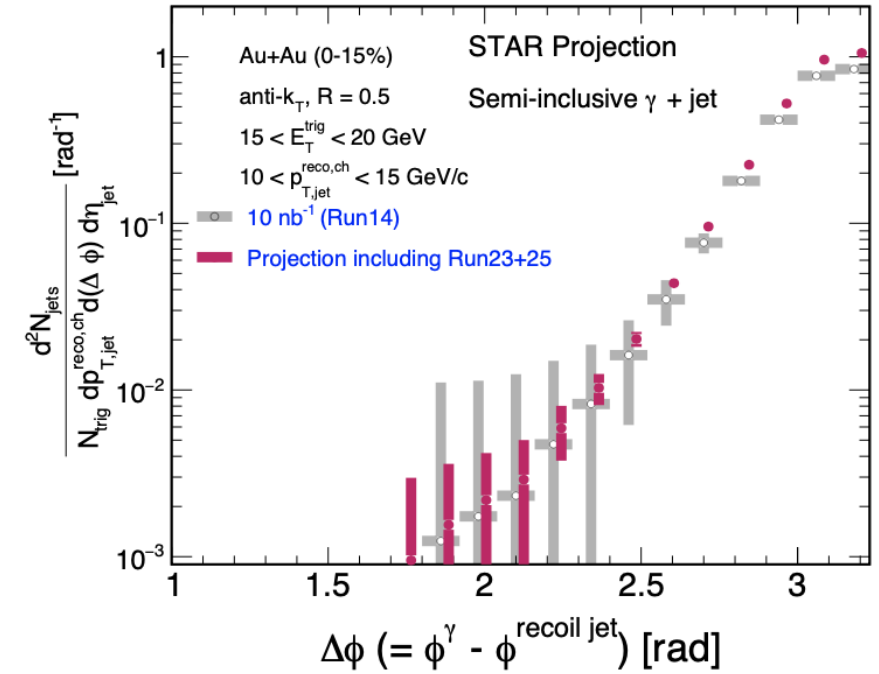


<https://www.bnl.gov/newsroom/news.php?a=122311>

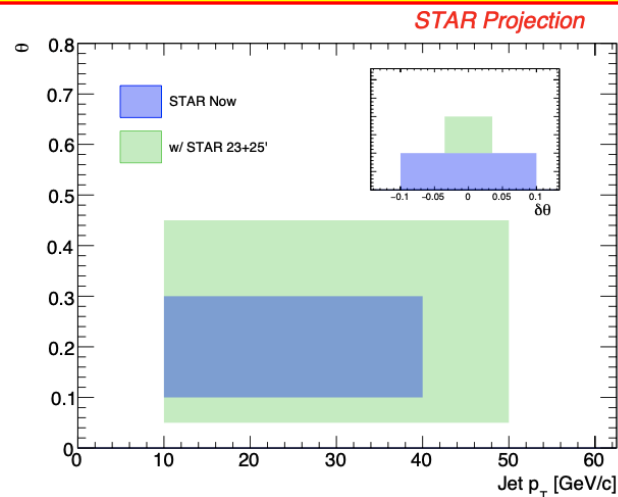
low p_T , large R, extended to higher p_T



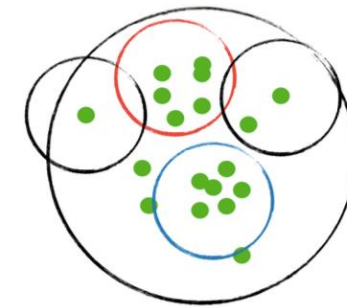
γ_{dir} +jet acoplanarity: constituents of medium



improved opening angle resolution by a factor of 4



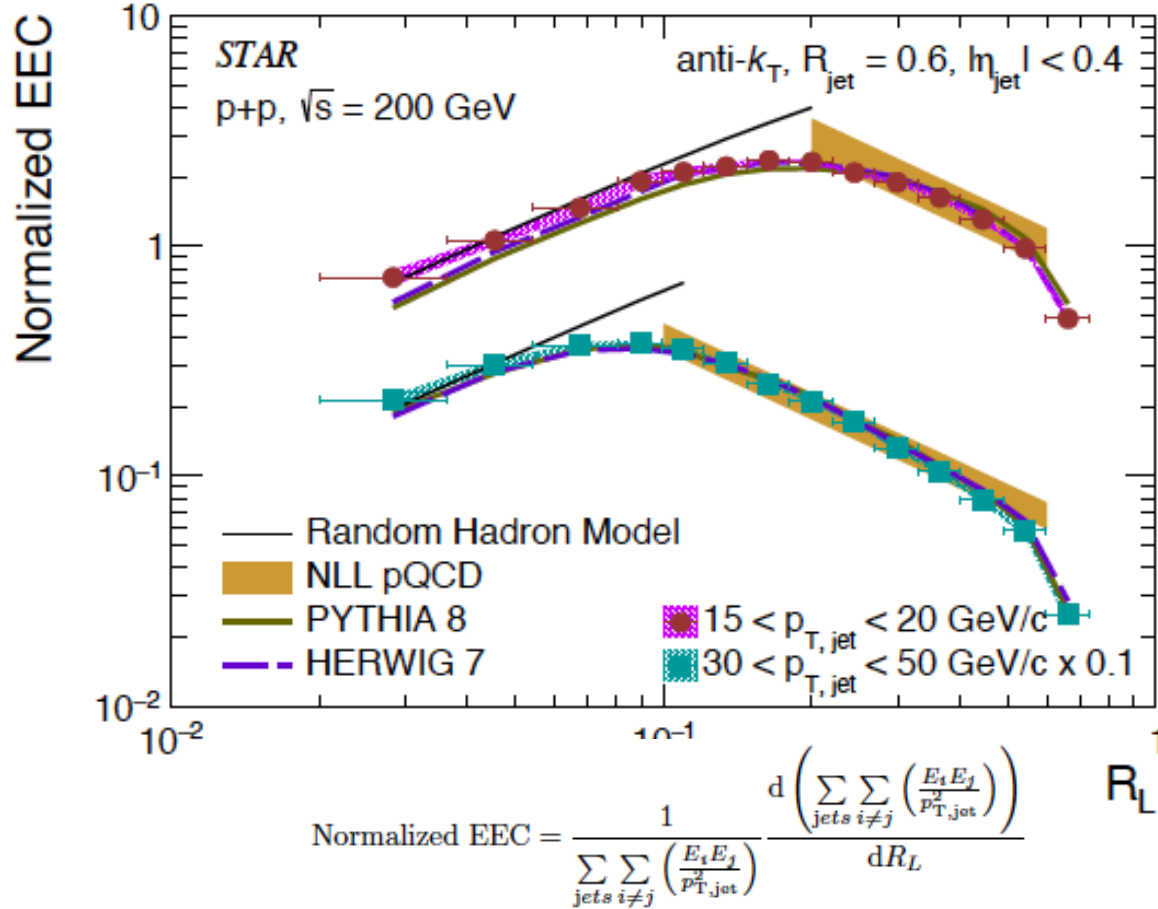
Jet substructure: coherence vs. de-coherence



Red: leading sub-jet
Blue: sub-leading sub-jet
 $Z_{SJ} = p_T^{blue} / (p_T^{blue} + p_T^{red})$
 $\theta_{SJ} = \Delta R(blue, red)$

Jet evolution and hadronization

arXiv: 2502.15925

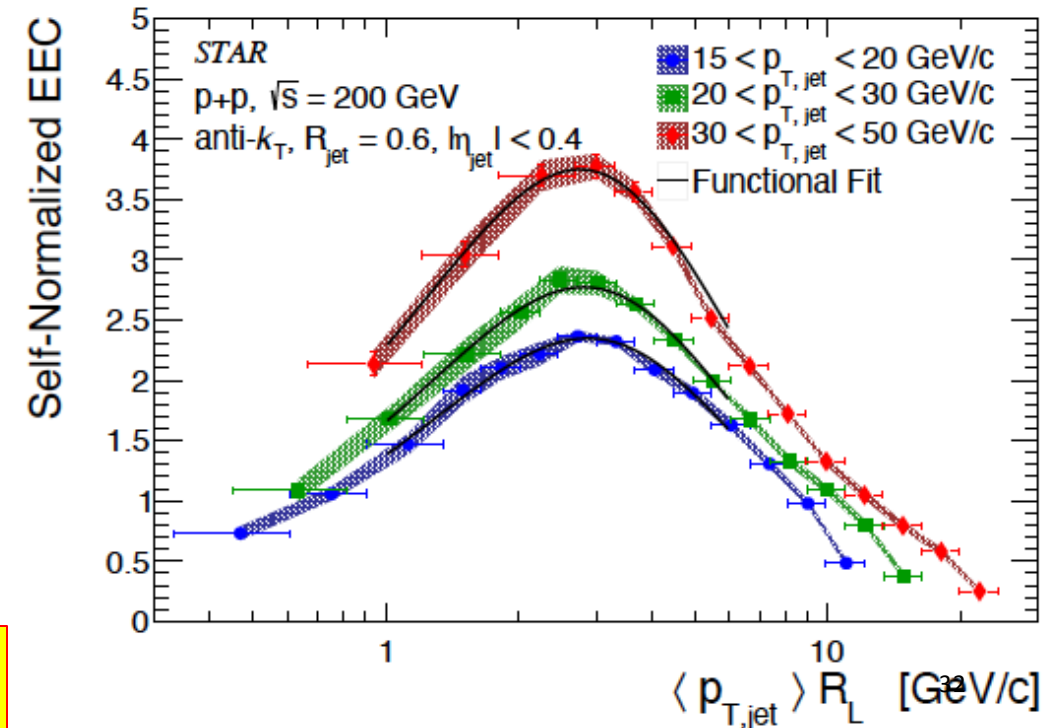


R_L : angular separation between two distinct tracks within a jet

- Heavy-Ion data will show modification at discrete angles
 - Onset of coherence
 - Diffusion wake

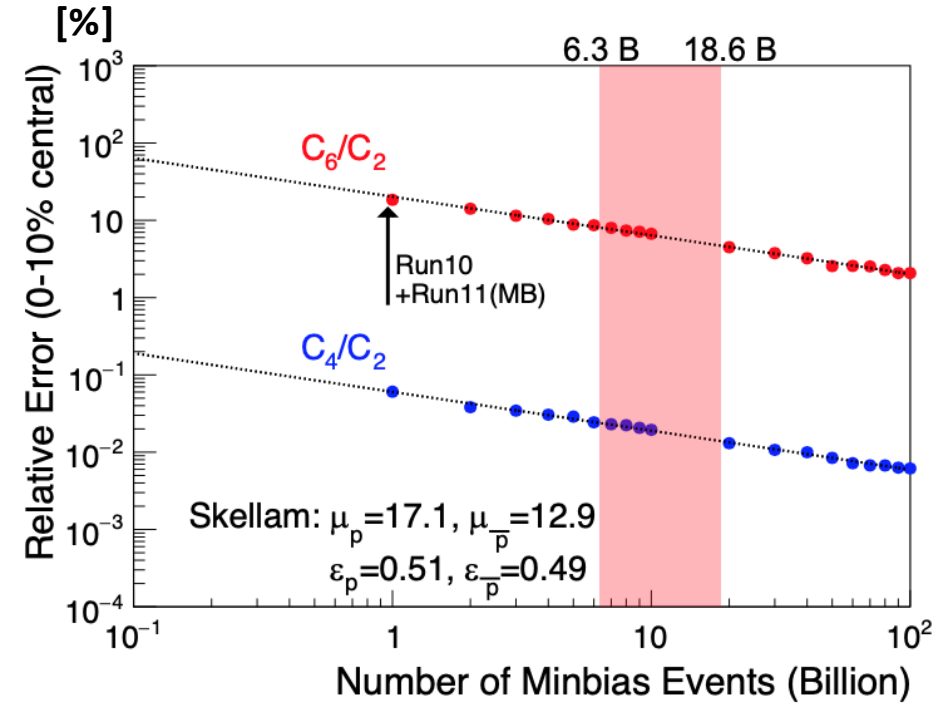
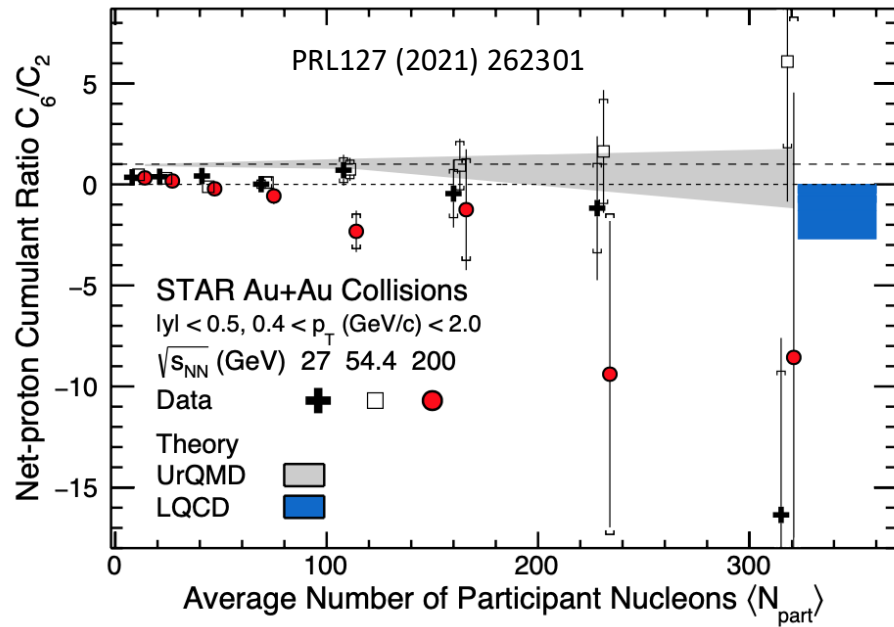
High statistics, improved opening angle and momentum resolution, unbiased centrality determination, forward and mid-rapidity comparisons

- Separates evolution of jet into angular regimes
 - Analyze both perturbative and non-perturbative
 - Locate transition between them – hadronization
- Peak moves as a function of jet momentum
 - Consistent transition regime within STAR
 - Dependent on initiator flavor – compare between experiments



Chiral cross-over transition

Improved PID, extended η coverage by iTPC



Lattice QCD predicts a sign change of susceptibility ratio χ_6^B/χ_2^B at T_c

The cumulants of net-proton distribution sensitive to chiral cross over transition at $\mu_B=0$

Observed a hint of a sign change from peripheral to central collisions at 200 GeV

$C_6/C_2 < 0$ at central collisions

High statistics measurements (10% statistical error for C_6/C_2 in central) will pin down the sign change

Discoveries of Breit-Wheeler process and vacuum birefringence

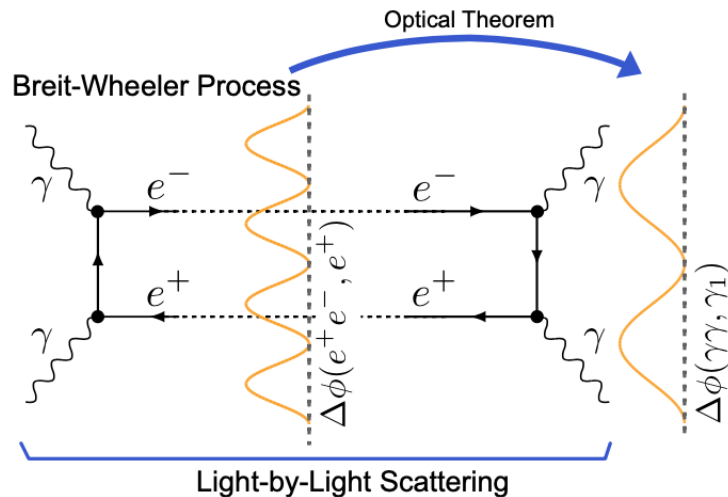
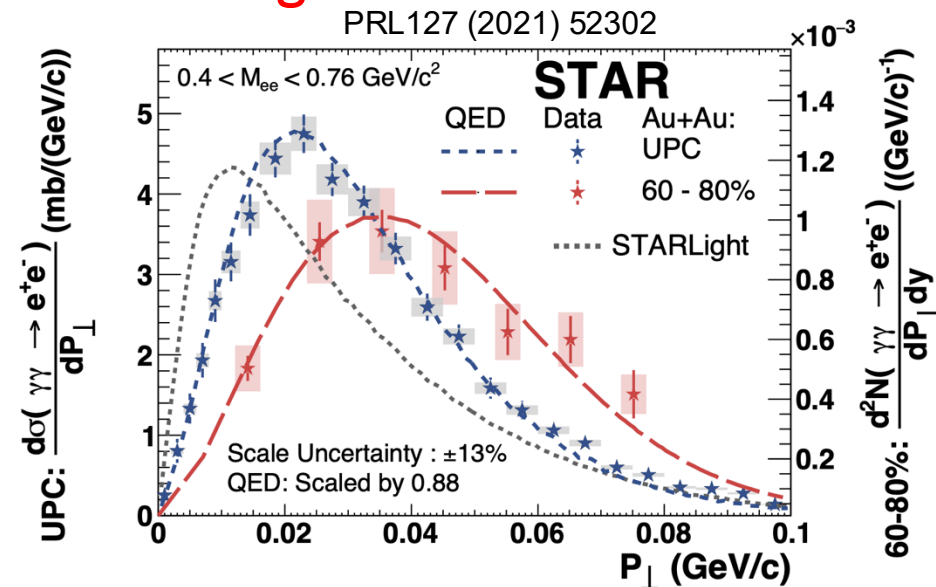
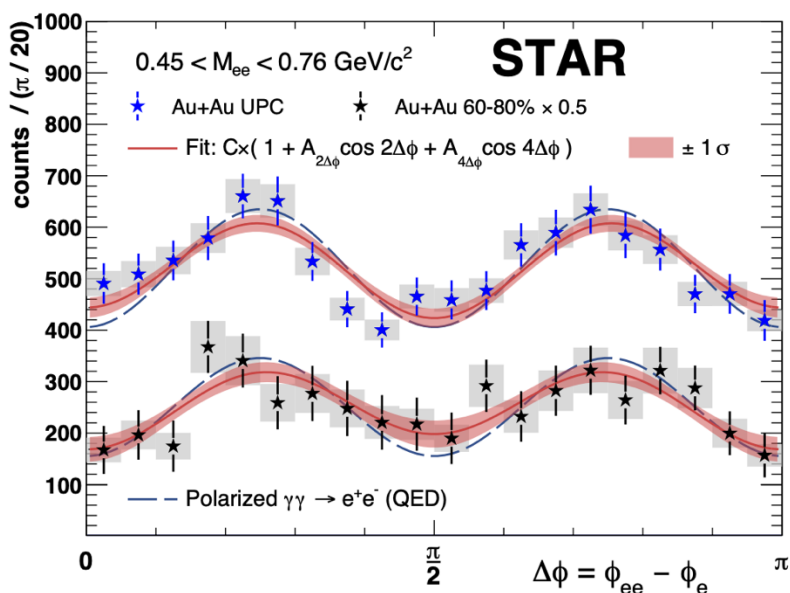


FIG. 1. A Feynman diagram for the exclusive Breit-Wheeler process and the related Light-by-Light scattering process illustrating the unique angular distribution predicted for each process due to the initial photon polarization.



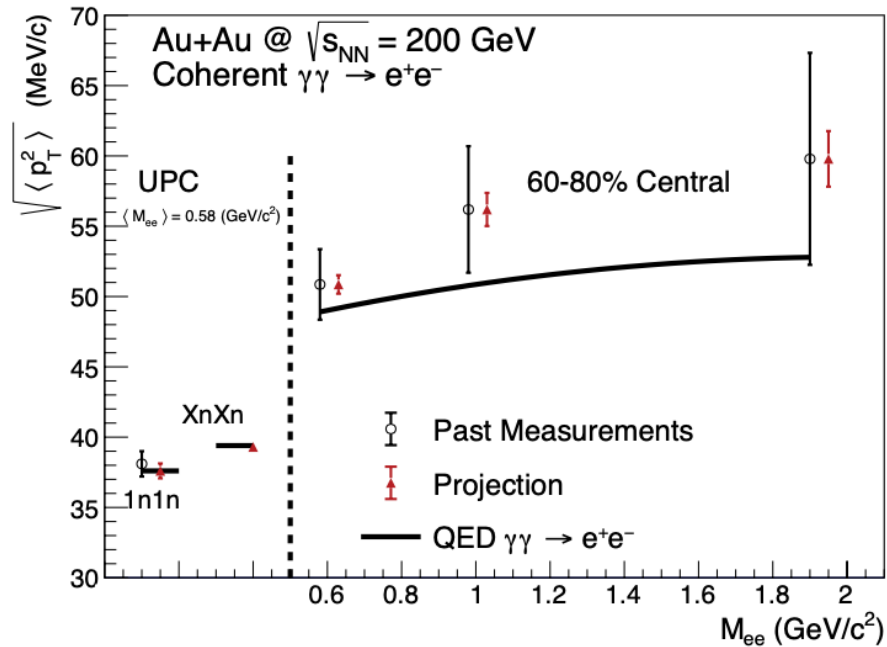
Observation of Breit-Wheeler process with all possible kinematic distributions (yields, M_{ee} , p_T , angle)

Dielectron p_T spectrum: broadened from large to small impact parameters

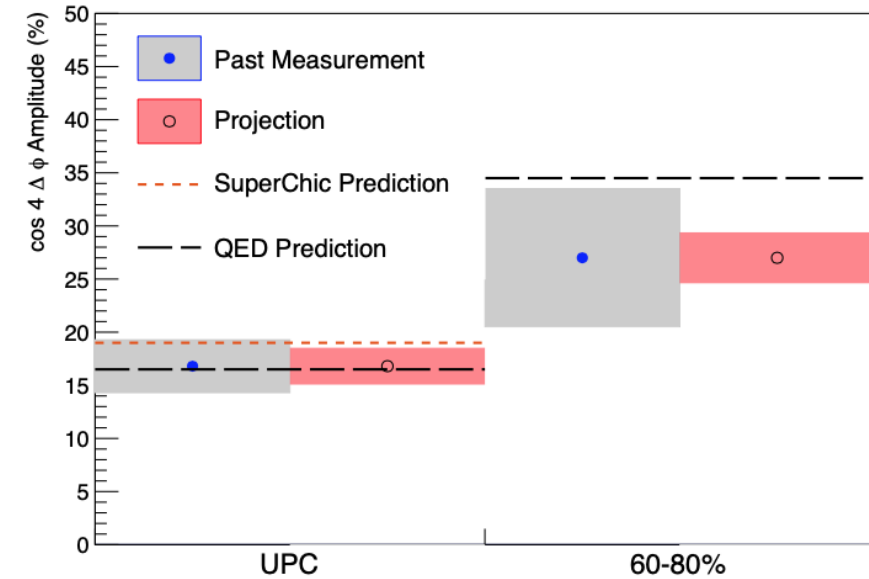
Observation of vacuum birefringence: 6.7σ in Ultra-peripheral collisions

Collisions of Light Produce Matter/Antimatter from Pure Energy:
<https://www.bnl.gov/newsroom/news.php?a=119023>

Photon Wigner function and magnetic effects in QGP



low material, improved PID, extended η and p_T coverage by iTPC



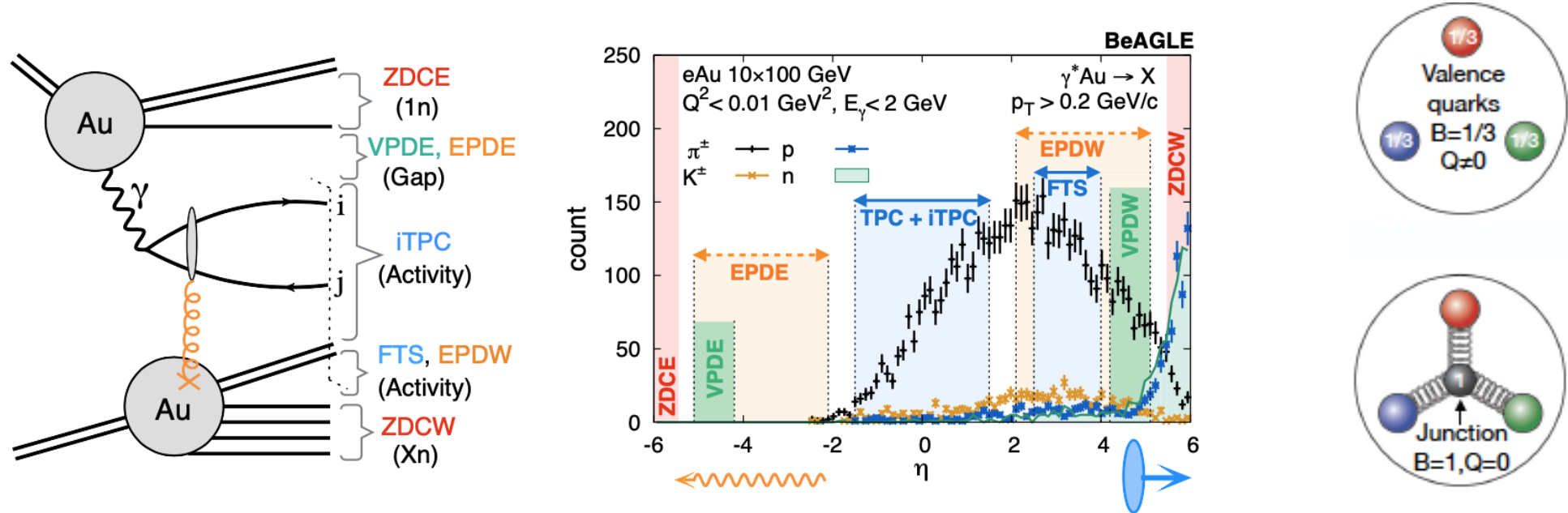
Impact parameter dependence of transverse momentum distribution of EM production is the key component to describe data; p_T broadening and azimuthal correlations of e^+e^- pairs sensitive to electro-magnetic (EM) field.

Is there a sensitivity to final magnetic field in QGP?

Precise measurement of p_T broadening and angular correlation will tell at $>3\sigma$ for each observable.

Fundamentally important and unique input to CME phenomenon.

Search for collectivity and signatures of baryon junction in photo-nuclear processes



γ +Au process in UPC associated with a large rapidity asymmetry:

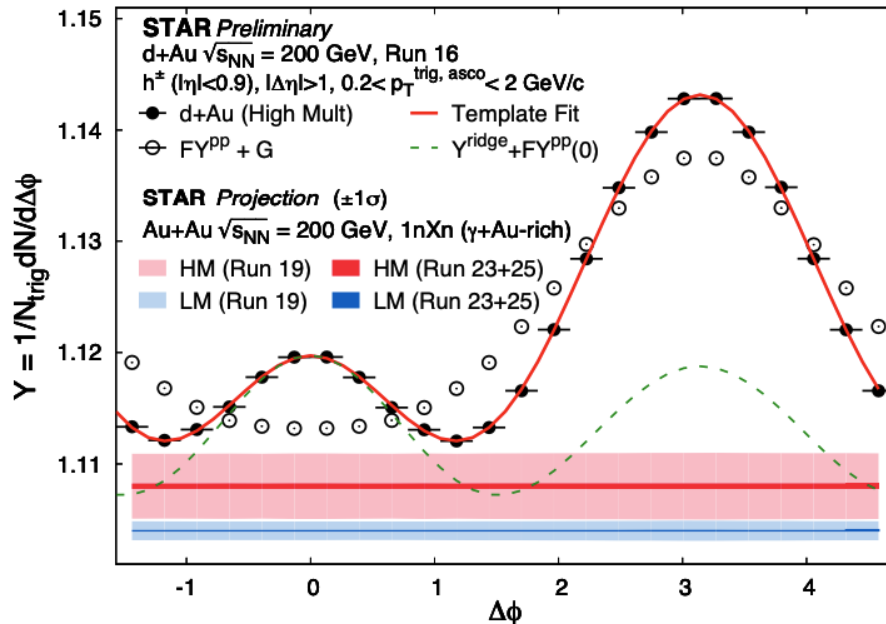
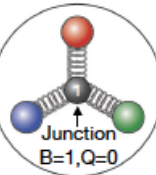
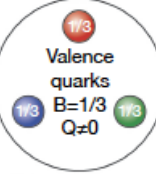
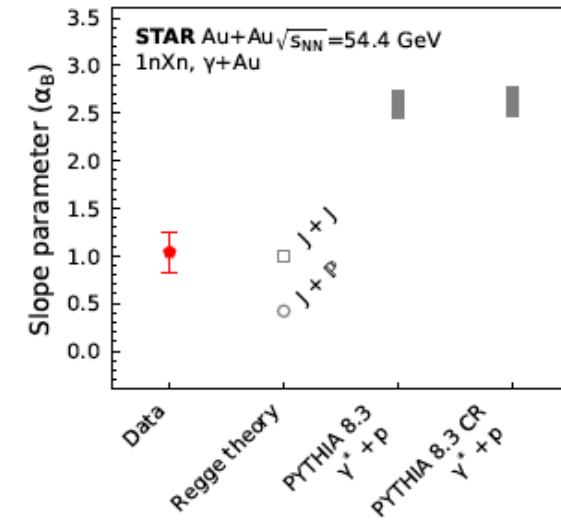
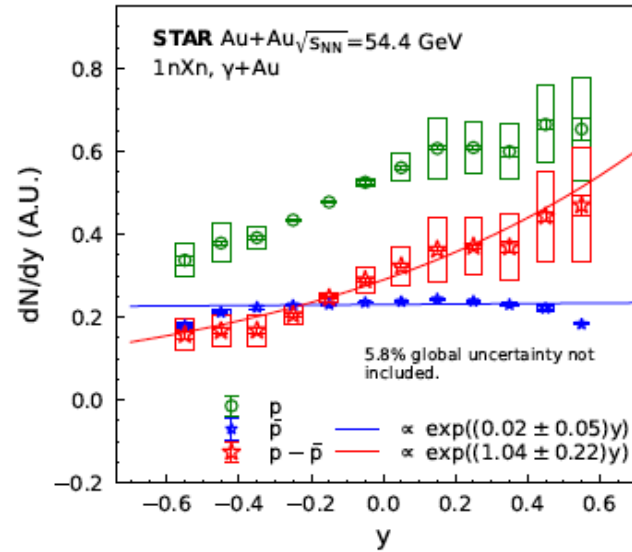
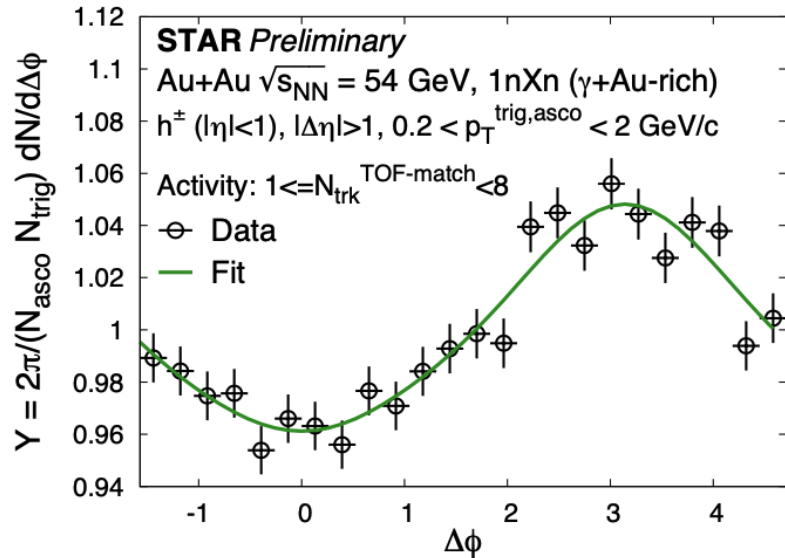
- Search for collectivity
- Study bulk observables

Further understand the origin of collectivity observed in small systems in addition to testing the baryon junction conjecture

Search for collectivity and signatures of baryon junction in photo-nuclear processes

improved PID, extended η coverage by iTPC, and forward tracking

arXiv: 2408.15441



γ +Au 54 GeV:

- No signature of collectivity
- Net-proton rapidity distribution consistent with the Regge theory prediction incorporating the baryon junction

Run23+25: enable differential measurements of di-hadron correlations

Search for collectivity in addition to testing the baryon junction conjecture

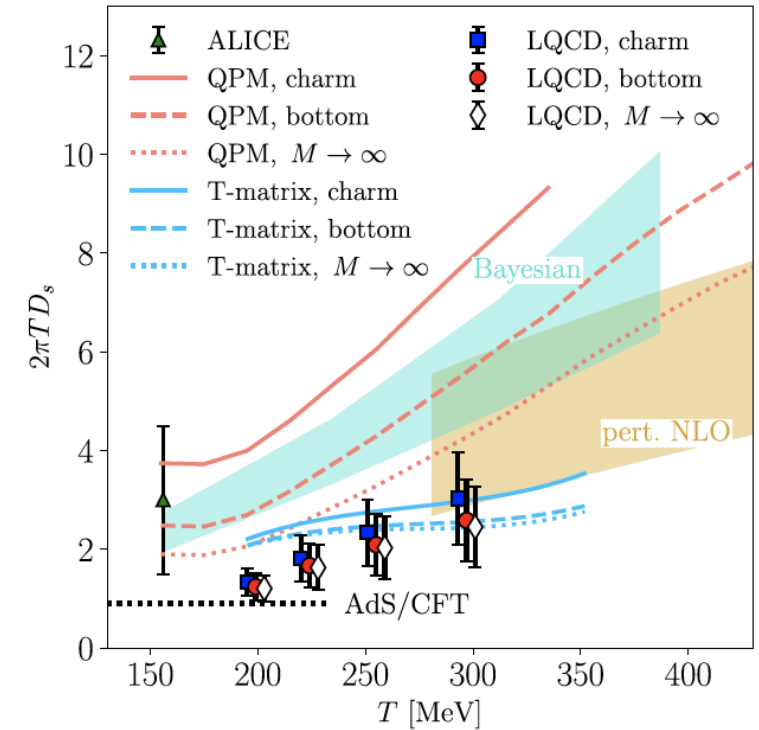
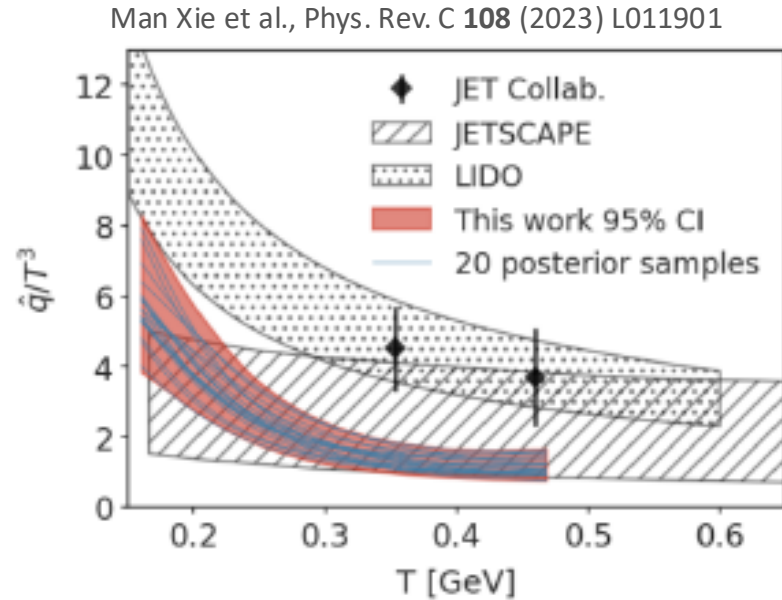
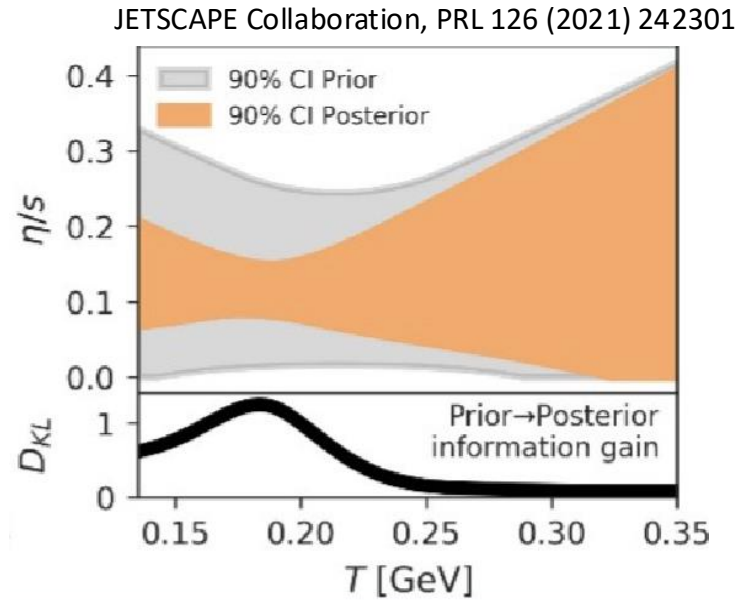
To address important questions about the inner workings of the QGP

- What is the nature of the 3-dimensional initial state at RHIC energies? r_n over a wide rapidity, J/ψ v_1 , photon Wigner distributions
- What is the precise temperature dependence of shear and bulk viscosity? v_n as a function of η
- What can be learned about confinement from charmonium measurements? J/ψ v_2
- What is the temperature of the medium? Different Υ states, $\psi(2S)$, thermal dileptons
- What are the electrical, magnetic, and chiral properties of the medium? Λ , Ξ , Ω P_H and K^* , ϕ , J/ψ ρ_{00} , thermal dileptons, CME observables
- What are the underlying mechanisms of jet quenching at RHIC energies? What do jet probes tell us about the microscopic structure of the QGP as a function of resolution scale? $\gamma_{\text{dir}}+\text{jet}$ I_{AA} , $\gamma_{\text{dir}}+\text{jet}$ acoplanarity, jet substructure
- What is the precise nature of the transition near $\mu_B=0$? Net-proton C_6/C_2
- What can we learn about the strong interaction? Correlation functions

To inform EIC physics with photon induced processes:

- Probe gluon distribution inside the nucleus: vector mesons (J/ψ), dijets (?)
- Search for collectivity and signatures of baryon junction: inclusive charge particles and cross sections, v_n , identified particle spectra

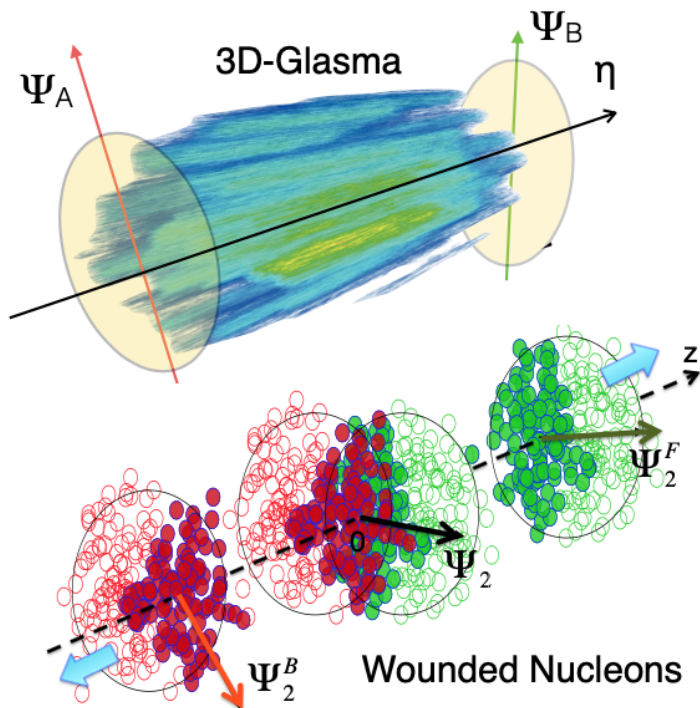
The future



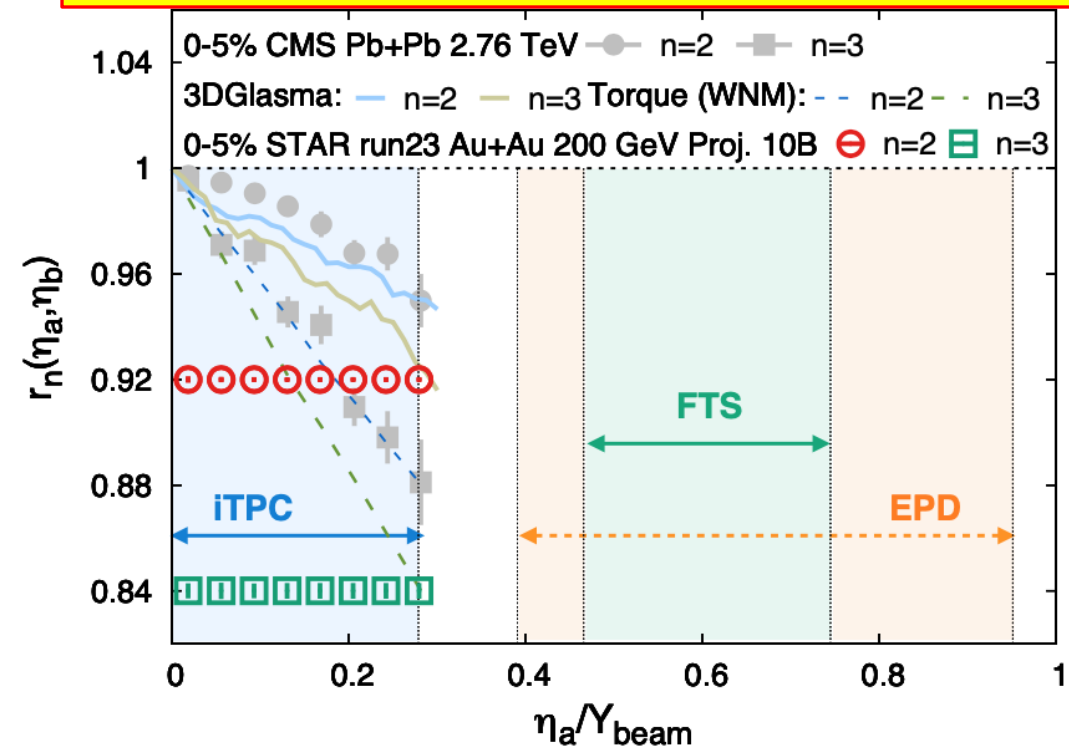
The newly built sPHENIX detector and upgraded STAR detector at RHIC, together with increased luminosity at the LHC and upgraded ALICE, ATLAS, CMS and LHCb detectors, will enable a multi-messenger era for hot QCD based on the combined constraining power of precise measurements using soft, hard, and electromagnetic probes. --> Establish a coherent picture of heavy ion collisions and inform properties of quark-gluon matter with strong theory collaboration.

Backup

Constrain longitudinal structure of initial state



extended η coverage by iTPC and forward tracking



$$r_n(\eta_a, \eta_b) = V_{n\Delta}(-\eta_a, \eta_b) / V_{n\Delta}(\eta_a, \eta_b)$$

$V_{n\Delta}$ the Fourier coefficient calculated with pairs of particles in different rapidity regions

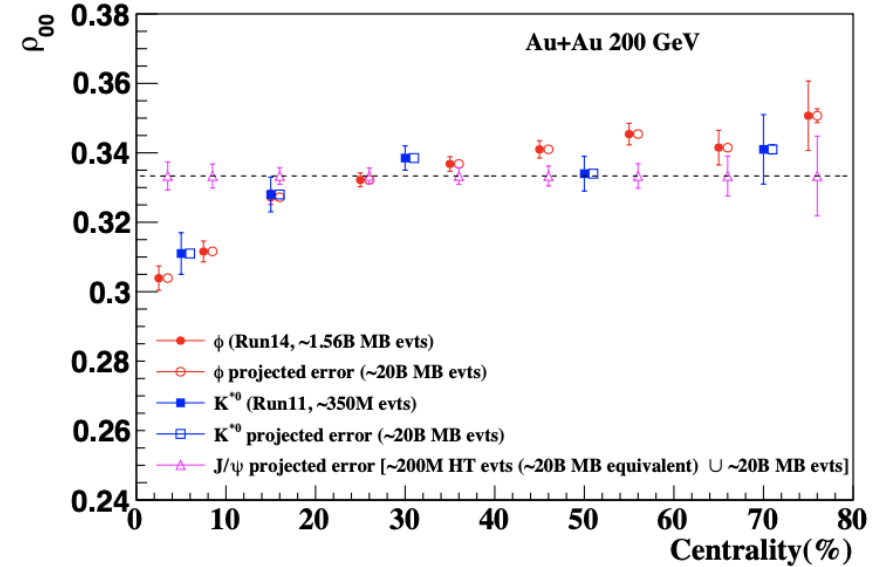
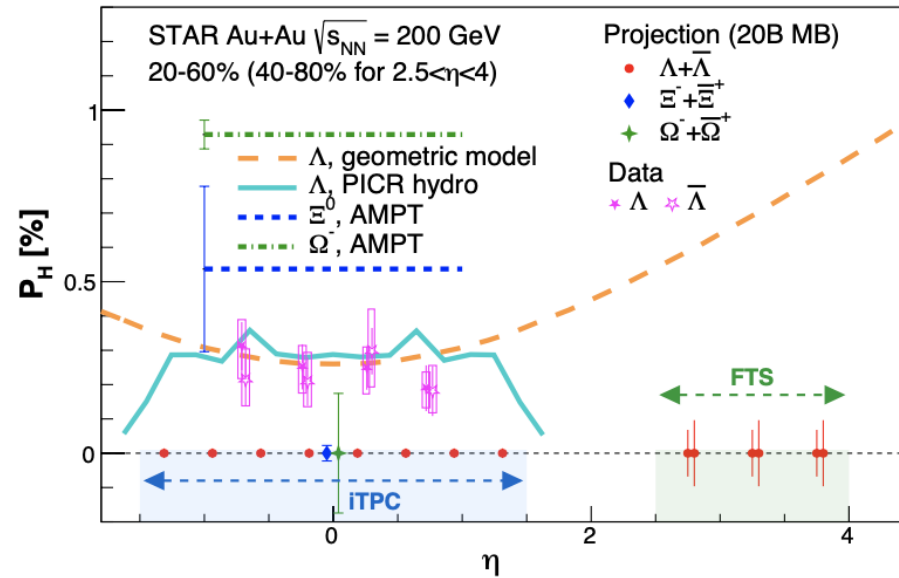
r_n sensitive to different initial state inputs:

- 3D glasma model: weaker decorrelation, describes CMS r_2 but not r_3
- Wounded nucleon model: stronger decorrelation than data

Precise measurement of r_n over a wide rapidity window will provide a stringent constraint

Global vorticity transfer

improved PID, extended η coverage by iTPC, and forward tracking



How exactly the global vorticity is dynamically transferred to fluid?

How does the local thermal vorticity of the fluid gets transferred to the spin angular momentum?

Rapidity dependence of Λ , Ξ , Ω P_H at STAR, probe the nature of global vorticity transfer:

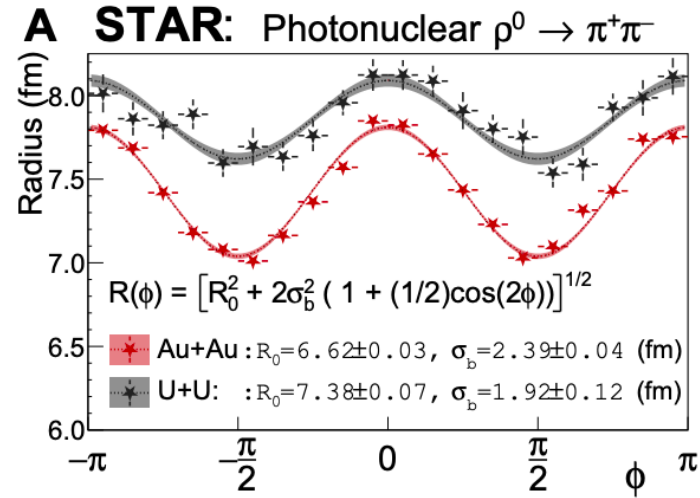
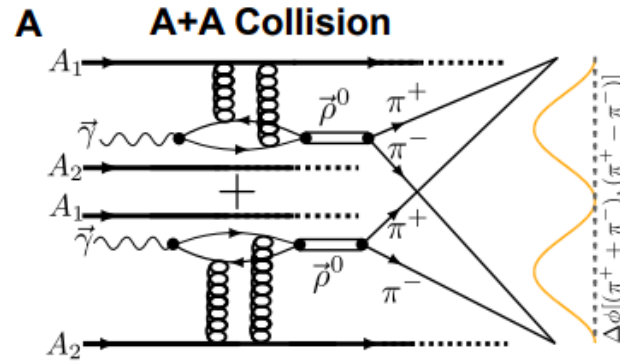
Initial geometry and local thermal vorticity + hydro predict opposite trends.

Can we reconcile P_H with vector meson spin alignment ρ_{00} ? Strong force field effect?

Precise measurements of ρ_{00} of K^* , ϕ , J/ψ will tell.

Tomography of ultra-relativistic nuclei with gamma + A collisions

Science Advances 9 (2023) 3903

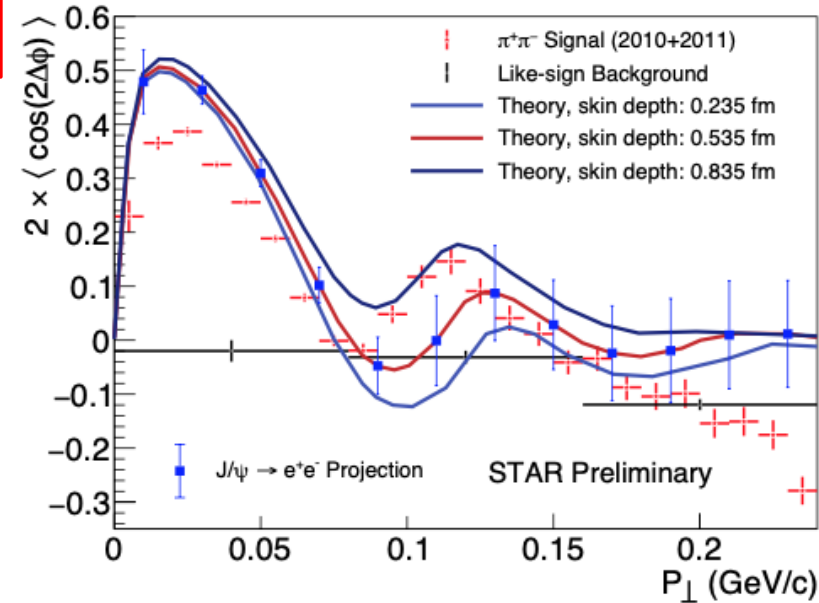
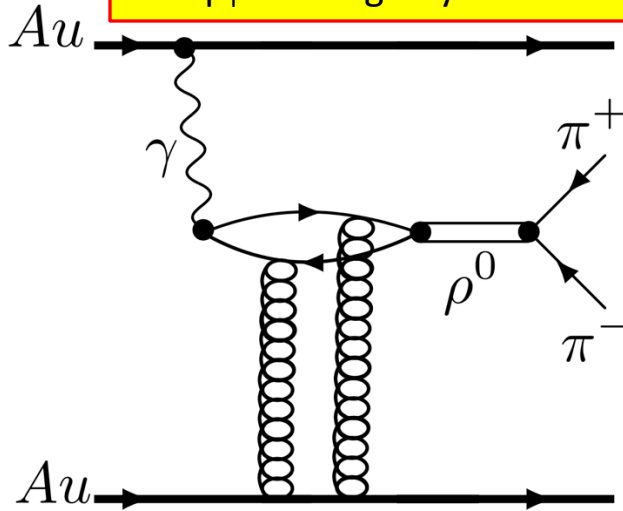


Quantum interference enabled nuclear tomography:

- A novel approach to extract the strong-interaction nuclear radii, which were found to be larger than the nuclear charge radii

Gluon distribution inside nucleus

low material, improved PID, extended η and p_T coverage by iTPC



Significant $\cos 2\Delta\phi$ azimuthal modulation in $\pi^+\pi^-$ pairs from photonuclear ρ^0 and continuum

Modulation vs. p_T , shows a diffractive pattern structure

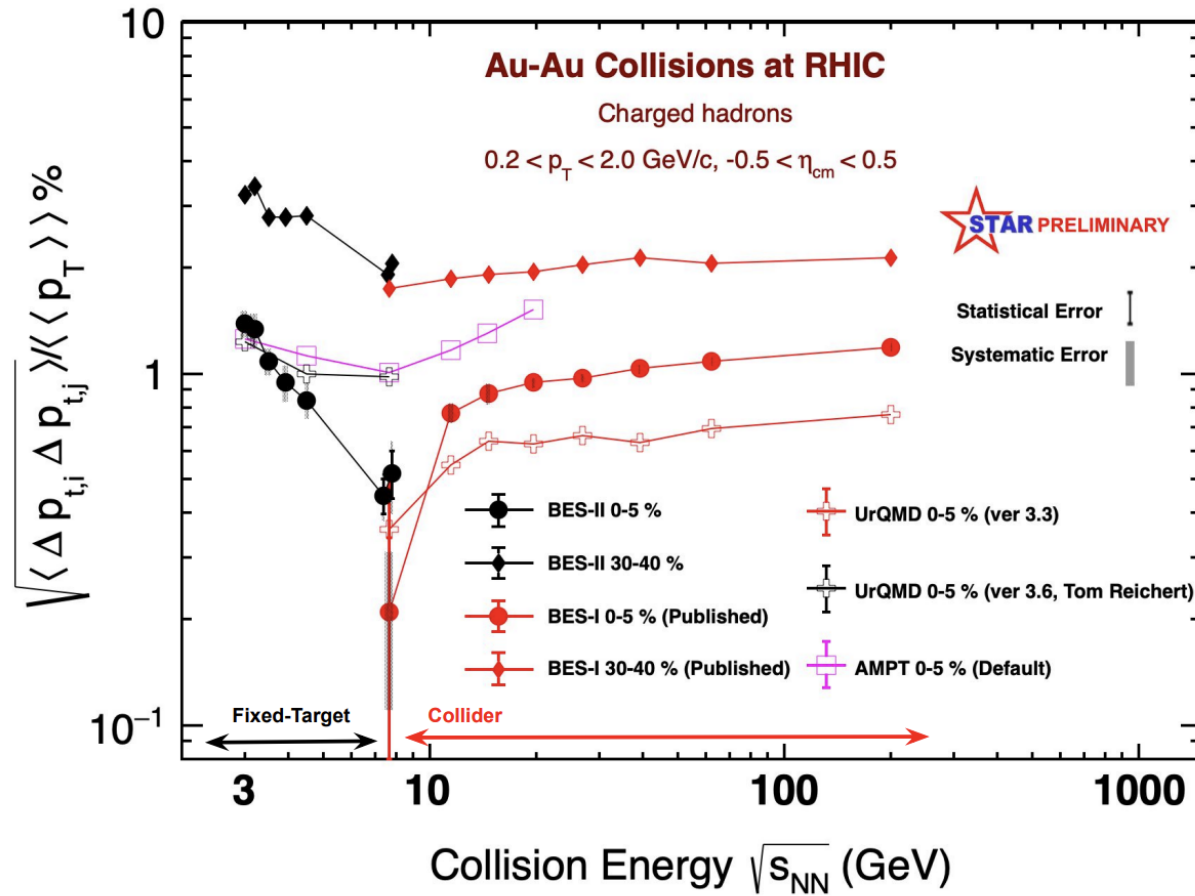
Theory (linear polarized photon + saturated gluons), sensitive to nuclear geometry and gluon distribution, closest to the gluon 3D tomography at EIC

Run23+25:

multi-differential measurements (vs. mass, rapidity, p_T): provide strong theoretical constraints, separate ρ^0 from continuum (Drell-Soding), investigate how double-slit interference mechanism affects the structure

Enable a similar measurement for J/ψ , a cleaner probe for gluon spatial distribution

Dynamical transverse momentum fluctuations



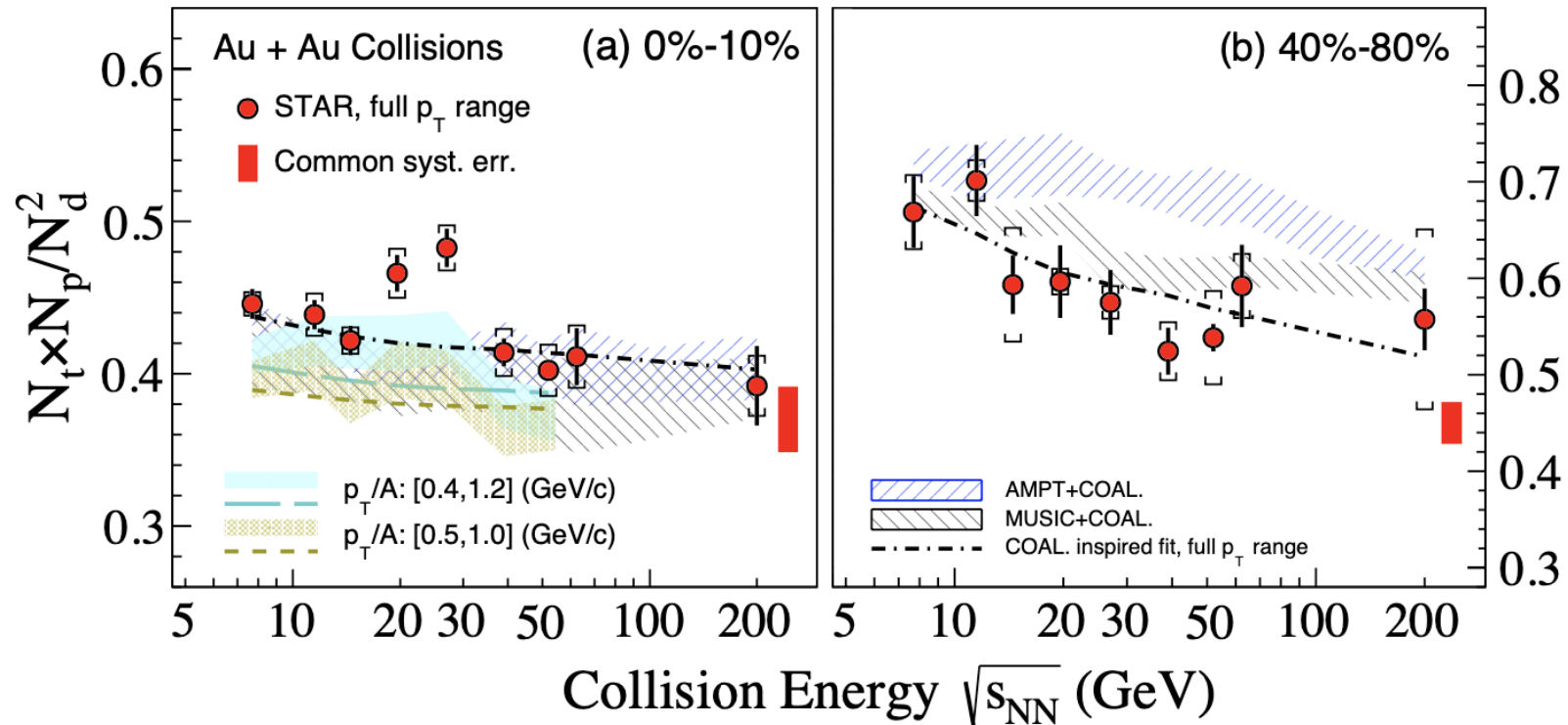
Non-monotonic energy dependence

To do:

- More comprehensive comparisons with baseline models

Light nuclei yield ratio

PRL 130 (2023) 202301



$N_t N_p / N_d^2$, **sensitive to fluctuations of the local neutron density** shows enhancements relative to the coalescence baseline with a significance of 2.3σ and 3.4σ respectively in 0 –10% central Au+Au collisions at 19.6 and 27 GeV.

Constrain production dynamics of light nuclei and understanding of the QCD phase diagram